Uncertainties in the land use flux resulting from land use change reconstructions and gross land transitions

Anita D. Bayer[1], Mats Lindeskog[2], Thomas A.M. Pugh[1,3], Richard Fuchs[4,5], Almut Arneth[1]

[1]Karlsruhe Institute of Technology KIT, Institute of Meteorology and Climate Research, Atmospheric Environmental Research, 82467 Garmisch-Partenkirchen, Germany.

[2]Department of Physical Geography and Ecosystem Science, Lund University, 223 62 Lund, Sweden.

[3]School of Geography, Earth & Environmental Science and Birmingham Institute of Forest Research, University of Birmingham, B15 2TT, United Kingdom.

[4]Wageningen University, Laboratory of Geoinformation Science and Remote Sensing, 6708PB Wageningen, the Netherlands.

[5]Environmental Geography Group, Department of Earth Sciences, Vrije Universiteit Amsterdam, De Boelelaan 1087, 1081 HV Amsterdam, the Netherlands.

Correspondence to: Anita D. Bayer (anita.bayer@kit.edu)

Abstract. Land-use and land-cover (LUC) changes are a key uncertainty when attributing changes in measured atmospheric CO_2 concentration to its sinks and sources, and must also be much better understood to determine possibilities for land-based climate change mitigation, especially in the light of human demand on other land-based resources. On the spatial scale typically used in terrestrial ecosystem models (0.5 or 1 degrees) changes in LUC over time periods of a few years or more can include bi-directional changes on the sub-grid level, such as the parallel expansion and abandonment of agricultural land (e.g. in shifting cultivation), or cropland-grassland conversion (and vice versa). These complex changes between classes within a gridcell have often been neglected in previous studies, and only net changes of land between natural vegetation cover, cropland and pastures accounted for, mainly because of a lack of reliable high-resolution historical information on gross land transitions. In the present study we applied a state-of-the-art dynamic global vegetation model with a detailed representation of croplands and carbon-nitrogen dynamics to quantify the uncertainty in terrestrial ecosystem carbon stocks and fluxes arising from the choice between net and gross representations of LUC. We used three frequently applied global and one recent European LUC datasets, two of which resolve gross land transitions, either in Europe or in tropical regions. When considering only net changes, land-use-transition uncertainties (expressed as one standard deviation around decadal means) in global carbon emissions from LUC (E_{LUC}) are ±0.23, ±0.76 and ±0.49 Pg C a^{-1} in the 1980s, 1990s and 2000s, respectively, or between 17 % and 42 % of mean E_{LUC}. Carbon stocks at the end of the 20th century vary by ±13 Pg C for vegetation and ±41 Pg C for soil C due to the choice of LUC reconstruction, i.e. around 3% of the respective C pools. Accounting for sub-grid (gross) land conversions significantly increased the effect of LUC on global and European carbon stocks and fluxes, most noticeably enhancing global cumulative E_{LUC} by 33 Pg C (1750-2014) and entailing a significant reduction in carbon stored in vegetation, although the effect on soil C stocks was limited. Simulations demonstrated that assessments of historical carbon stocks and fluxes are highly uncertain due to the choice of LUC reconstruction and that the consideration of different contrasting LUC reconstructions is needed to account for this uncertainty. The analysis of gross in addition to net land changes showed that the full complexity of gross land-use changes is required in order to accurately predict the magnitude of LUC change emissions. This introduces technical challenges to the process-based models and relies on extensive information on historical land use transitions.

Keywords: land-use change, gross land transitions, land-use flux

1. Introduction

Under a growing population's increasing demand for food and fiber, as well as for bioenergy, greater anthropogenic pressures on the global land area are expected. Today, carbon dioxide (CO_2) emissions resulting from to land-use and land-cover (LUC) change are the second largest contributor to anthropogenic emissions to the atmosphere after fossil fuel combustion (Le Quéré et al., 2015), and they are a term that is associated with large uncertainties. LUC and their changes include the processes when land is converted from one land-cover type to another (e.g. the conversion of forest to cropland or grasslands to pastures), and the effects from LUC related to the management of the land, such as e.g. cropping practices, fertilizer use, irrigation and different types of tillage. LUC changes affect the cycling of carbon (C), energy, water and other nutrients (phosphorous, nitrogen), in many cases enhancing greenhouse gas (e.g. CO_2, N_2O, CH_4) emissions from agricultural soils and pastures when compared to natural vegetation and altering species composition. These changes go hand-in-hand with altered characteristics such as surface albedo, surface aerodynamic roughness and rooting depth (Pongratz et al., 2010).

Conversions from natural vegetation to croplands and pastures generally reduce C stored in vegetation (Baccini et al., 2012), decrease soil C stocks in croplands but not in pastures (Guo and Gifford, 2002; McLauchlan, 2006) and, unless fertilized, reduce soil nitrogen (N) pools (McLauchlan, 2006). The alteration of C and N pools is mainly a result of initial deforestation and of the decreased litter input due to biomass extraction upon harvest and accelerated soil decomposition rates, the latter being stimulated through management practices such as tillage or a changed microclimate at the soil surface. However, in some regions croplands show increased C sequestration potential compared to the natural vegetation owing to enhanced growth under improved agricultural practices including fertilization and irrigation (Ciais et al., 2010; Schulze et al., 2010). Legacy fluxes can change C due to e.g., an imbalance between reduced litter input and decomposing dead biomass and affect LUC emissions over decades or more (Gasser and Ciais, 2013; Houghton, 2010; Krause et al., 2016; Pugh et al., 2015). During vegetation recovery on abandoned agricultural land, secondary land ecosystems sequester C due to regrowing vegetation and re-accumulation of C in soils. These LUC-related processes determining regional sources and sinks of C entailed a global total net C flux to the atmosphere over the past centuries (deB Richter and Houghton, 2011; Houghton et al., 2012; McGuire et al., 2001; Le Quéré et al., 2015).

A number of studies have recently highlighted the importance of different definitions when assessing the net carbon flux from LUC (E_{LUC}) related to the fact that in different studies different LUC component-fluxes are included in the overall E_{LUC} calculation (Gasser and Ciais, 2013; Pongratz et al., 2014). Likewise, it is important to consider whether or not historical effects of environmental change are included in assessments of cleared C stocks as part of E_{LUC}. Less focus so far has been put on the explicit datasets of historical land use employed (Le Quéré et al., 2013). A limited number of historic LUC reconstructions are available at global scale, mostly at 0.5° resolution (Hurtt et al., 2011; Kaplan et al., 2012; Klein Goldewijk et al., 2011; Olofsson and Hickler, 2008; Pongratz et al., 2008; Ramankutty and Foley, 1999), two of which are very similar (Hurtt et al., 2011; Klein Goldewijk et al., 2011). At continental scale some higher resolution reconstructions exist for instance for Europe (Fuchs et al., 2015b; Kaplan et al., 2009; Williams, 2000). Most reconstruction approaches combine information on current and recent historical LUC from national statistics with estimates of global population distribution and growth as the main driver of historical LUC. Model assumptions are made to fill data gaps and extrapolate the available information to create subnational patterns, and therefore large uncertainties arise both from the original data sources and modeling assumptions (see, e.g. Klein Goldewijk and Verburg, 2013). However, reconstructions on continental scales are able to use a more data-driven approach (e.g. Fuchs et al., 2013, 2015c) compared to global land reconstructions, since the data availability is often better for these study areas.

Most historical LUC reconstructions focus on the difference in net area under natural, cropland or pasture vegetation cover in a grid location between two time steps (net land changes) instead of explicitly showing the sum of the absolute value of all land transitions occurring on a sub-grid scale (gross land changes). In particular over coarser grid-resolutions, gross land-cover changes allow a deeper view of LUC, tracking land conversion events such as the parallel expansion and abandonment of agricultural land, e.g. as in shifting cultivation (cycle of cutting forest for agriculture and abandoning it after some years of usage, followed by a period of fallow with regrowing forests). This entails altered biogeochemical dynamics within different sub-sections of a gridcell, e.g. secondary land acts as a C sink during vegetation regrowth, while additional land clearing leads to relatively

rapid loss of C stocks in vegetation and soils, along with other changes in vegetation composition, nutrients and biogeophysical properties (e.g. Houghton et al., 2012). Accounting in ecosystem models separately for the effects of e.g., 10% of an area converted from natural vegetation to cropland while another 10% of cropland is abandoned for regrowth over the same time period therefore will lead to a very different response of ecosystem states and fluxes compared to the effects of net changes, which in this case would be zero.

The availability of land-use information including gross land transitions is limited due to a lack of reliable historical information determining these. However, a few data sets exist representing gross land transitions, such as the dataset by Hurtt et al. (2011) who provide model estimates of tropical shifting cultivation on global scale based on assumed land rotation rates. Fuchs et al. (2015b) recently estimated gross land changes for Europe over the 20th century based on empirical evidence. As the number of gross land transitions can greatly exceed the number of net transitions at spatial resolutions typically employed for global studies, neglecting these can lead to a serious underestimation of LUC dynamics with implications for biogeochemical, ecological and environmental assessments (Fuchs et al., 2015a, 2015b; Stocker et al., 2014; Wilkenskjeld et al., 2014). Earlier studies revealed significant differences when ecosystem C dynamics were simulated when accounting for gross land changes in areas of shifting cultivation in addition to net changes as specified by Hurtt et al. (2011) (e.g. Shevliakova et al., 2013; Stocker et al., 2014; Wilkenskjeld et al., 2014). Others have implemented their own assumptions on spatial distribution and rotation scheme under shifting cultivation and combined these with C-cycle calculations (Olofsson and Hickler, 2008; Stocker et al., 2014).

In this study we use a state-of-the-art dynamic global vegetation model (DGVM) to calculate ecosystem C stocks and fluxes in response to different LUC reconstructions, (1) to explore the consistency of different LUC representations and to quantify the uncertainty in ecosystem C stocks and fluxes, including E_{LUC}, resulting from the different reconstructions, and (2) to quantify the effect of accounting for gross land transitions in addition to net changes in LUC. We use four historical LUC reconstructions, three of which are global and one is for the European domain. One of the global datasets represents gross transitions with shifting cultivation in tropical regions, and the European dataset represents gross transitions in Europe. We apply a model with representation of LUC and changes therein, including a number of crop functional types and C-N dynamics in natural vegetation and crops. We exclude wood harvest as a form of forest management from our analysis as its parameterization is poorly constrained on a global scale, e.g. the effects strongly depend on assumptions regarding turnover times of harvested C (Wilkenskjeld et al., 2014).

2. Methods
2.1. Land-use datasets

For the global scale, three historical LUC datasets were selected that are frequently used for ecosystem modeling studies. These datasets run from 1700 to present and are also the basis for future LUC scenarios (e.g. van Asselen and Verburg, 2013; Hurtt et al., 2011). For Europe we additionally considered one recently published dataset running from 1900-2010. Table S1 provides an overview of the LUC datasets and their characteristics.

Ramankutty and Foley (1999) (RAMA) published changes in cropland area for the period 1700 to 1992 in 5 min global resolution. The dataset was built based on historical cropland inventory data at national and subnational levels in combination with a remote-sensing derived cropland map for 1992. The algorithm to hindcast LUC distributed the historical cropland area within political units, i.e. the 1992 cropland areas are scaled for each political unit so that the cropland total matches historical inventory data. Therefore, the reconstructed changes in historical croplands are consistent with the history of human settlement and patterns of economic developments, although they do not resolve changes in LUC dynamics below the smallest spatial entity in the inventory data. Natural vegetation was calculated as the residual of cropland and pasture area. The analysis was revised in 2012 so that it also accounts for pasture areas and the dataset was extended until 2007 in 0.5° x 0.5° spatial resolution (Ramankutty, 2012). Natural areas are now the remainder of cropland and pasture areas. Here we apply the revised 0.5° x 0.5° version.

The History Database of the Global Environment (HYDE) 3.1.1 (Klein Goldewijk et al., 2010, 2011) provides spatially gridded maps of cropland and pastures at 5 min resolution for the period 10 000 BC to AD 2000. Here, historical population data and national and sub-national statistics of change in agricultural area (mainly the United Nations Food and Agriculture Organization, FAO, supplemented with numerous other statistics) were
145   combined to a land-use per capita relationship. Land use was then allocated for present day based on satellite-derived land cover for 2000 and for the past by a combination of this base map with a number of weighting and suitability factors such as population density and habitat information on soil suitability, distance to rivers, slopes etc. Temporal resolution is 10 years for the historical period after 1700 and annual after 2000. The HYDE dataset used here was extended until 2013 in the annual carbon budget analysis (Le Quéré et al., 2015).

150   The Hurtt et al. (2011) Land Use Harmonization (LUH) database is for the historical period (1500-2005) based on the land-use data of HYDE 3.1 (Klein Goldewijk et al., 2010, 2011) and combines these with national statistics of historical wood harvest and assumptions regarding shifting cultivation in tropical regions. Additional assumptions were made regarding the prioritization of land for conversion and logging, the wood harvest spatial patterns and the residence time of land in agricultural use in shifting cultivation areas. LUH data provide
155   fractional data on cropland, pasture, primary and secondary vegetation as well as gross transitions between land-use states based on shifting cultivation in tropical regions on 0.5° x 0.5° spatial resolution. Secondary land is defined as natural land that was previously used for agriculture and is recovering from this disturbance. Shifting cultivation is implemented as bi-directional LUC change with an assumed rotation period of 15 years, corresponding to an annual turnover rate of 6.7 % of the area (Hurtt et al., 2011). Although the history of shifting
160   cultivation is not known, it is today present mainly in tropical regions and therefore in the LUH dataset it is limited to tropical regions for the historical period (Fig. S1**Fehler! Verweisquelle konnte nicht gefunden werden.**, Olofsson and Hickler, 2008). The LUH dataset was extended until 2014 in the annual carbon budget analysis (Le Quéré et al., 2015). As LUH is a modeled product that is based closely on the HYDE database, these products were reported to be relatively similar (Hurtt et al., 2011).

165   The newest LUC dataset considered here, the HIstoric Land Dynamics Assessment (Fuchs et al., 2013, 2015b), reconstructs gross and net land changes for the EU27 (EU from 2007-2013) plus Switzerland at 1 km spatial resolution (Fig. S1). Net land conversions are based on national statistics. To account for gross changes, empirical evidence (mostly time series of large-area LUC maps and national surveys) on historic gross LUC changes was aggregated to derive an overall gross/net ratio per LUC class and a relative weighted land
170   conversion matrix which were applied to national net change data. Gross changes are derived by calculating the difference between two time steps of the gross land change reconstruction. The allocation of LUC fractions to grid cells was done based on probability maps for each LUC class, forest volume stock maps and large-scale historic LUC maps (Fuchs et al., 2015c). An aggregated version of the CORINE 2000 land-cover dataset was used as base map for the year 2000. The initial LUC dataset that was built based on empirical evidence covers
175   1950-2010 in decadal steps but was extrapolated back to 1900 to assess the long-term impacts of changes in LUC. For each time step the 1 km grid cells were classified as being dominated by settlement, cropland, forest, grassland (incl. managed pastures), other land (glaciers, sparsely vegetated areas, beaches and water bodies) or water. Here, we consider only the gross LUC reconstruction of HILDA (Fuchs et al., 2015b) and derive net LUC changes from gross land transitions. In the original HILDA net LUC reconstruction (Fuchs et al., 2015b) the
180   results differ spatially from our net reconstruction due to the use of different land allocation mechanisms under net and gross changes in their analysis.

2.2. LPJ-GUESS ecosystem model

We use the LPJ-GUESS DGVM (Sitch et al., 2003; Smith et al., 2001) with updates for land-use change (Lindeskog et al., 2013) and C-N coupling in natural vegetation and crops (Olin et al., 2015; Smith et al., 2014)
185   allowing for the simulation of nitrogen limitation on plant and crop development. Three distinct land-use types are used (natural vegetation, pasture and cropland) with natural vegetation modeled by 9 woody and 2 grass plant functional types (PFTs) (as in Smith et al., 2014), which are distinguished in terms of their bioclimatic preferences, photosynthetic pathways and growth strategies. Croplands are represented by three crop functional types that are parameterized using information on summer wheat, winter wheat and maize, and with crop-
190   specific processes including dedicated carbon allocation and phenology, explicit sowing and harvest

representation, irrigation, fertilization and cover crops (Olin et al., 2015). Pastures are modeled using competing C3 and C4 grass PFTs, where each year 50 % of the C and 12.5 % of the N in above-ground biomass was removed as a representation of grazing (Krause et al., 2016; Lindeskog et al., 2013).

In LPJ-GUESS, upon conversion of natural land to cropland and pastures, the natural vegetation is cleared and
195   97% of wood (stem wood 65%, branches and coarse roots 32%) and 10% of leaf biomass is harvested. Out of the harvested stem wood, one third goes to a product pool with a turnover time of 25 years. The rest of the harvested biomass is oxidized and released to the atmosphere, while the remaining biomass enters the litter pool (see Lindeskog et al., 2013). In reductions of the natural vegetation area, young stands (but older than 15 years, the assumed rotation period in shifting cultivation by Hurtt et al., 2011) are converted before older stands. Following
200   agricultural abandonment, natural vegetation recolonizes the land in a typical succession from herbaceous to woody plants, if environmental conditions are suitable for tree growth. Competition for resources and light among age cohorts of woody PFTs is simulated directly through gap dynamics (see, e.g. Bugmann, 2001).

The model has been evaluated extensively and has demonstrated skills in capturing large-scale vegetation patterns (Hickler et al., 2006, 2012) and dynamics of the terrestrial carbon cycle (Ahlström et al., 2012; Morales
205   et al., 2005; Olin et al., 2015; Piao et al., 2013; Pugh et al., 2015; Smith et al., 2014). The carbon flux response was shown to be close to the ensemble mean in a recent intercomparison of nine dynamic global vegetation models (Sitch et al., 2015).

2.3.   Simulation protocol

LPJ-GUESSS was run at 0.5° x 0.5° resolution with simulations beginning in year 1700 . CRU TS 3.21
210   historical global climate data (University of East Anglia Climatic Research Unit (CRU), 2013) was used for the period 1901-2014. 1700-1900 climate data was provided by repeating 1901-1930 CRU climate with de-trended temperature data. Atmospheric CO_2 forcing was provided from observations from ice-cores and, later in the 20th century, atmospheric measurements (Tans and Keeling, 2015), with a value of 286.4 ppmv used from 1700 until the beginning of this dataset in 1860, and a final atmospheric concentration of 396.7 ppmv in 2014. Simulations
215   were spun-up for 500 years using land-use fractions and CO_2 mixing ratio from the first simulation year, and de-trended climate data of the first 30 simulation years, with a longer spin-up for soil carbon pools (see Smith et al., 2014). Model spin-up was therefore identical for net and gross land changes. In order to assign cropland areas to crop functional types, global crop cover fraction was partitioned based on Portmann et al. (2010), and mapped to LPJ-GUESS crop types, as described in Olin et al. (2015). Crop type fractions were held constant throughout the
220   simulations. Where cropland was expanded into a hitherto un-cropped grid cell, average CFT fractions of the nearest neighboring cropland cells were used to populate it. Past values of global nitrogen deposition was taken from simulations from Lamarque et al. (2010 and 2011) and nitrogen fertilization of crops was estimated as in Zaehle et al. (2011). LPJ-GUESS simulations are summarized in Table 1.

Global simulations starting in 1700 were carried out using the three net and one gross LUC dataset (LUH net,
225   RAMA net, HYDE net, LUH gross), and for Europe starting in 1900 using two net and one gross LUC dataset (HILDA net, LUH net, HILDA gross). For these, all LUC input data were aggregated to 0.5° spatial resolution and decadal HILDA and HYDE LUC data were interpolated linearly to annual time steps. Although some of these LUC products represent changes between forested and non-forested land, in the simulations done here, only the changes between the classes croplands, pastures, natural vegetation and barren land (available for LUH
230   and HILDA) were considered; the composition of natural vegetation was simulated directly by LPJ-GUESS. Primary and secondary vegetation as in LUH (wood harvest), and the forest class in HILDA were represented by natural vegetation. The HILDA LUC classes of settlements, water and other land were aggregated to the LUC class barren. The grassland class in HILDA comprises both pastures, meadows and natural grasslands, but was used for pastures, a reasonable assumption for Europe due to the small area of truly natural, unmanaged
235   grassland in Europe (Wilkins et al., 2003). For global simulations a land mask was used that includes only cells of the ice-free land area for which all three global LUC datasets provide data (58 790 cells). For the EU, all 0.5° grids that contained at least one HILDA cell were used (2 486 cells).

We examine differences caused by the different LUC reconstructions on net land-use flux (E_{LUC}), deforestation flux, net primary productivity (NPP), and ecosystem C stocks in vegetation and soils. E_{LUC} is calculated as the
240   difference between a model simulation with transient historical LUC change (gross or net LUC change) and a simulation with constant LUC distribution as in the first simulation year (Table 1, LUC fixed to 1700/1900). All

simulations are driven by varying climate, atmospheric CO_2 mixing ratio, N deposition and N fertilization (see, e.g. Le Quéré et al., 2015; Pongratz et al., 2014). This method includes effects of LUC and changes therein interacting with climate and atmospheric CO_2, and is consistent with definition 1 of Gasser and Ciais (2013) and D3 of Pongratz et al. (2014). In the same way, the effect of accounting for LUC on NPP and C stocks in vegetation and soils was calculated as the difference between the simulation with gross or net LUC changes and the respective reference simulation. Soil C includes both C in soils and litter. The deforestation flux is the C released upon land conversion only. In the calculation of net cumulative E_{LUC} for global simulations the first 50 simulation years were ignored because of high carbon fluxes in the first decades of gross simulations, which reflected a re-equilibration under LUC including gross transition rates (i.e. shifting cultivation) that were not part of model spin-up, and effectively reflect emissions from shifting cultivation that occurred before 1700 (see, e.g., Stocker et al., 2014). Because gross transitions in Europe do not follow a systematic rotation such as shifting cultivation areas in the global simulations, this effect is not so directly applicable here and cumulative E_{LUC} was calculated starting in 1900. We restrict our analysis to the global scale, which has direct relevance for the global carbon budget; a detailed analysis of regional differences and processes is beyond the scope of this study.

3. Results
3.1. Historical land transitions

The most pronounced change in global vegetation cover over the historical period is the deforestation of natural areas for conversion into croplands and pastures (Fig. 1a), progressing at fairly low rates during the first decades after 1700, followed by a steadily increasing trend from about 1860 until a slow-down and stabilization sets in after about 1960. Total land area transitions before 1850 (Fig. 1c) are below 0.1×10^6 km^2 a^{-1}, from which they steadily increase with a rate of additional ca. $6\,400 \pm 1\,100$ km^2 a^{-1} under transition each year (average of three LUC datasets 1850-1960). Transitions in all three LUC reconstructions peak between 1950 and 1960 when deforestation due to expansion of agriculture in the tropics and pasture expansion in grass and shrub dominated biomes was highest in the LUC reconstructions (Fig. S2). After the 1960s all three LUC reconstructions assume continued deforestation in the tropics at a lower rate and reforestation in Europe and some parts in Northern America following the abandonment of agricultural areas. Transitions around 1960 are believed to be influenced by the LUC reconstruction process, when model assumptions for the historical period before 1960 are merged with the records of the Food and Agriculture (FAO) records available thereafter.

The three global net LUC datasets applied here differ primarily in the total area of pasture and natural vegetation and in the regions in which these are located, with RAMA generally forming the median in terms of global absolute area under natural LUC among the three LUC reconstructions, but with a higher agreement of spatial patterns between LUH and HYDE. Major differences occur in eastern Africa, eastern Europe and the southern parts of Russia (maps not shown). After 1960, LUH and HYDE are very similar (showing major differences only in Australia). While the deforestation trend is shown by all three global LUC reconstructions, the absolute loss rates of natural vegetation differ, with HYDE being 12 % above numbers estimated in LUH and 22 % above RAMA (Table 2). For present-day, differences are largest in natural areas and pastures, with RAMA reporting about 6 % more natural areas and about 8 % less pasture areas in 2007 compared to LUH and HYDE (Fig. 1a, Table 2). Differences in pasture areas occur worldwide, but are somewhat higher in Saudi-Arabia, western China, Mongolia and Australia (maps not shown). Before 1950 differences in natural and pasture area between LUH/HYDE and RAMA exist predominantly in eastern Europe, southern parts of Russia and eastern Africa.

In Europe historical LUC included the expansion of areas with regrowing natural vegetation after 1900 following land abandonment as a result of intensification on high production cropland (Fig. 1b). Net gain in natural regrowth area from 1900 to 2010 is about 6×10^5 km^2 (average of two LUC datasets, Table 3). Rates of total land conversion in Europe over the first half of the 20th century (Fig. 1d) remain at a fairly constant level, with between 10 000 and 15 000 km^2 being converted each year. Rates of land conversion are only higher between 1950 and 1970.

The European land-use reconstruction HILDA shows the same trend in LUC over the historical period when compared with the same domain extracted from the global LUH product (Fig. 1b) but the two datasets disagree

notably with respect to the absolute area of natural vegetation and pastures (Table 3). HILDA shows substantially larger fractions of pasture than LUH especially in Scandinavia and southern Europe, while LUH shows higher pasture fractions than HILDA in central Europe and the Baltic area. The higher areas of pasture in HILDA may result from the fact that natural grasslands are included in the pasture class in HILDA but not in the
295   pasture class of LUH (see methods). The peak in total land conversion rates around mid of the century is shown in HILDA in two steps with slightly higher rates in 1950s and a maximum in the 1960s (13 700 and 19 100 km^2 per year) and in LUH in one step with a more than doubled rate in the 1950s compared to the previous decades (on average about 42 600 km^2 per year). From 1950 to 1960 the LUH dataset shows a rapid decrease in pasture area of 1.5 x 10^5 km^2 that is mainly reflected in a significant gain in natural areas.

300   **3.2. Effects of different net LUC changes on carbon pools and fluxes**

In LPJ-GUESS simulations all three global net LUC reconstructions resulted in similar projections of the land-use change flux E_{LUC} as a source of C on the global scale, with the rate of emission accelerating from the early 1800s (Fig. 2a). Reflecting the time-series of the land transitions (Fig. 1c), E_{LUC} peaked in the 1950s with emissions of about 2.0 to 2.6 Pg C a^{-1}. Mean E_{LUC} was 1.2, 2.0 and 2.1 Pg C a^{-1} for LUH, RAMA and HYDE,
305   respectively, at the end of the historical period (1998-2007, Table 2) and cumulative E_{LUC} since 1750 was between 210 Pg C for LUH and 225 and 229 Pg C for HYDE and RAMA, respectively, in 2007 (Fig. 2b, Table 2). From the three reconstructions, projections based on HYDE resulted in the lowest emissions until the early 1900s, probably because of the lowest conversion of natural areas to pastures until this period compared to the other reconstructions (Fig. 1a). Also when using the HYDE product, a second peak of E_{LUC} of around 2.7 Pg C a^{-}
310   ^{1} occurred in the late 1990s (15-year average) that is not seen in LUH and RAMA reconstructions (between 1.0 and 1.6 Pg C a^{-1} in this period).

Global average NPP was simulated to increase strongly over the last century due to the effect of higher vegetation productivity under increased atmospheric CO_2 mixing ratio and (in cool areas) climate warming. Compared to reference simulations with LUC fixed in 1700 (red lines in Fig. 2d), all three LUC representations
315   showed a reduced increase in NPP over the duration of the simulations (Table 2, Fig. S3), with the reduction due to LUC at the end of the historical period (averages 1998-2007) being 1.9 Pg C for LUH, 2.4 Pg C for HYDE and 3.3 Pg C for RAMA LUC reconstructions (Table 2). Global total and time-series of NPP simulated with the three LUC reconstructions was very similar for RAMA and HYDE, and was about 2 Pg C lower for LUH simulations for the entire simulation period (Fig. 2d) as a result of a higher pasture area instead of natural
320   (woody) vegetation in the LUH data in the African extra-tropical regions and areas in eastern Europe and southern Russia.

For global C stocks both in vegetation and soils the positive trend induced by CO_2 fertilized vegetation growth (red lines in Fig. 2e and f) was counteracted by the effects of LUC change. A minimum of vegetation C stocks during the simulation period was simulated for all LUC reconstructions in the 1960s when LUC reduced
325   vegetation C stocks on average by 111 Pg C (Table 2) compared to the reference simulations. Following the decline in conversion rates of natural into managed land thereafter, vegetation C stocks increased in response to vegetation productivity responding to the fertilizing effect of increasing atmospheric CO_2 concentration. Vegetation C stocks at the beginning of the simulation period were similar for RAMA and HYDE reconstructions with about 496 Pg C, but on average about 31 Pg C lower for LUH simulations because of the
330   lower natural area in this dataset (Table 2).

Time-trends in soil C stocks over the simulation period followed similar trends as vegetation C stocks, albeit with a 5- to 10-year time lag (Fig. 2e, f). Loss in soil C as a result of accounting for LUC was a direct effect of the removal of biomass upon harvest reducing litter input in the following years and the increase in soil C decomposition rates associated with tillage. On average 75 Pg soil C were lost due to changes in LUC in the
335   2000s with only a small variation of ±1 Pg C between the three LUC reconstructions (Table 2). Overall soil C stocks were again very similar for RAMA and HYDE (average 1 514 Pg C) and only about 68 Pg C lower for LUH at the beginning of the simulation period (Fig. 2e, Table 2).

In Europe, LUC caused emission of C until the 1960s, but turned into a sink thereafter (Fig. 3a, negative E_{LUC}) as a result of the reduction of pastures and also croplands in the second half of the last century and the regrowth of

340   natural (woody) vegetation (Fig. 1b). This development is shown in simulations with both HILDA and LUH, however the magnitude of the effect of LUC on C stocks and fluxes was somewhat stronger in simulations applying the LUH dataset, due to a higher deforestation rate in LUH until the 1950s (Fig. 3c, absolute land transitions were similar for both LUC datasets, Fig. 1d). To this sense, E_{LUC} decreases from about 19 Tg C a^{-1} (HILDA) and 38 Tg C a^{-1} (LUH) in the 1900s to about -52 Tg C a^{-1} for HILDA and -80 Tg C a^{-1} for LUH in the
345   2000s and cumulative E_{LUC} from 1900 to 2010 was -936 Tg C for HILDA and -1 890 Tg C for LUH (Table 3).

Same as in the global simulations, also for Europe a positive trend in NPP was simulated from 1900 that is linked to increasing CO_2 fertilization (Fig. 3d). Accounting for changes in LUC reduced NPP in simulations applying HILDA by 57 Tg C a^{-1} but only slightly changed NPP in the 2000s when applying LUH (increase of 10 Tg C a^{-1}, Table 3) because of highly productive croplands in central Europe (Fig. S4a). NPP simulated with
350   HILDA was between 50 and 100 Tg C a^{-1} lower over the simulation period than simulated with LUH (Table 3), also a result of the lower share, and therefore productivity, of natural areas in HILDA as opposed to pastures.

Similar trends in vegetation and soil C were simulated with both datasets, with changes dominated by deforestation over the first decades and reforestation thereafter (see Fig. 1b). In the 2000s vegetation C stocks were even higher under net LUC changes compared to the respective reference simulations (Table 3). C stocks in
355   vegetation of simulations using LUH were on average about 2 000 Tg C and 25 % higher than simulations applying HILDA (Fig. 3e, Table 3). Differences in soil C stocks between the two LUC representations were small, with soil C being about 1 900 Tg C higher in LUH simulations (3 % of soil C stocks projected with HILDA) at the beginning of the simulation period (Table 3). In comparison to the trend in C stored in vegetation, stocks in soils only increased from the 1950s on. Effects of LUC on C stocks in vegetation and soils were
360   stronger for simulations applying LUH (Fig. 3e), showing increases in both C stocks in central and Eastern Europe but decreases in southern countries (Fig. S4b, c).

3.3.   Global and European effects of accounting for gross land transitions

The global land area undergoing LUC when considering gross land transitions based on the LUH dataset (Fig. 1c) was 4.7 times the net area converted (total transitions 1700-2014, Table 2), with all additional land
365   transitions in this dataset being generated by shifting cultivating in the tropics (Fig. S1a). This increased the global land-use flux E_{LUC} by about 0.14 Pg C a^{-1} to 1.64 Pg C a^{-1} at the end of the historical period (2005-2014 average flux) and resulted in cumulative E_{LUC} being 33 Pg C higher in 2014 for gross compared to net LUC simulations (Fig. 2a, b, Table 2). Global NPP was 1.5 Pg C a^{-1} (i.e. 3 %) lower in simulations of gross land changes compared to the net simulations (Fig. 2d, Table 2), which was an effect of lower mean levels of forest
370   canopy closure in areas subject to shifting cultivation in the tropics. For the same reason, the reduction of vegetation C stocks as an effect of accounting for gross effects was high with 35 Pg C, i.e. -8 %, at the end of the simulation period and with 11 Pg C low for soil C stocks compared to the absolute size of soil C stocks (-0.8 %, 2005-2014, Fig. 2e and f, Table 2). The reduction of vegetation C stocks by the effects of LUC changes further increased by 24 % when accounting for gross LUC and for soil C stocks by 14 % (2005-2014, Table 2).

375   For Europe, the HILDA gross dataset predicted land transitions (Fig. 1d) that were about 1.4 times higher when accounting for gross transitions relative to net LUC changes (total transitions 1900-2010, Table 3) (see also Fuchs et al., 2015b) with significant gross land changes occurring all over Europe (Fig. S1b). As a result, gross E_{LUC} was enhanced, compared to net, by about 11 Tg C a^{-1} in the beginning of the simulation period (1901-1910). Cumulative gross E_{LUC} was -531 Tg C in 2010, or 406 Tg C higher than E_{LUC} under net LUC transitions (-
380   936 Tg C), representing a reduced cumulative sink as the result of higher previous emissions from LUC when considering gross transitions (Fig. 3b, Table 3). NPP was also lower in gross simulations, however differences were small (-18 Tg C a^{-1}, see Table 3) and the gross simulation followed the same trend as the net LUC simulation. For C stocks on European level the difference between net and gross simulations was -158 Tg C for vegetation carbon and -254 Tg C for soil C stocks at the end of the simulation period (2001-2010, Fig. 3e and f,
385   Table 3).

4. Discussion

4.1. Uncertainties in carbon stocks and fluxes due to the choice of historical LUC reconstruction

390   It is widely acknowledged that a key uncertainty in estimating changes in C stocks and fluxes as a response to LUC change stems from the choice of the LUC dataset (e.g. Houghton et al., 2012; Jain et al., 2013). With a detailed representation of succession when natural vegetation recolonizes abandoned agricultural lands, the representation of croplands by a number of crop functional types and the consideration of C-N interaction in natural vegetation and crops, the LPJ-GUESS model considers key processes and interactions that are crucial

395   when accurate estimates of C stocks and fluxes are derived based on detailed dynamics on LUC (see, e.g., Hickler et al., 2004; Lindeskog et al., 2013; Olin et al., 2015; Pugh et al., 2015; Zaehle, 2013).

Uncertainties in E_{LUC} resulting from the choice of LUC reconstruction (expressed as one standard deviation around decadal means) quantified with the LPJ-GUESS model and the three global net LUC data sets in the 1980s, 1990s and 2000s were ±0.23, ±0.76 and ±0.49 Pg C a^{-1} (17 %, 42 % and 28 % of E_{LUC}), respectively (see

400   Table 2 for exact periods). Among the three datasets, E_{LUC} using LUH and RAMA were similar, with HYDE differing somewhat from these resulting from regional differences in croplands (e.g. HYDE showing less croplands in Northeastern US around 1900). Uncertainties confirmed estimates from previous studies in which a subset of the three LUC hindcasts (partially as earlier versions) were applied, sometimes in combination with a book-keeping method (**Fehler! Verweisquelle konnte nicht gefunden werden.**). Previously, uncertainties

405   were estimated for the 1980s with ±0.30 Pg C a^{-1} from the synthesis experiment of Houghton et al. (2012), and for the 1990s with ±0.20 Pg C a^{-1} found by Shevliakova et al. (2009) when using HYDE and RAMA cropland data (in earlier versions, including wood harvest). For the 2000s Jain et al. (2013) found an uncertainty of ±0.21 Pg C a^{-1} when quantifying E_{LUC} with HYDE and RAMA datasets with a coupled C-N model and also the book-keeping approach from Houghton (2008). Our uncertainty of E_{LUC} due to the choice of LUC reconstruction was

410   higher in the 1990s, where especially E_{LUC} derived using HYDE data was significantly higher due to a strong increase in pastures (Fig. 2a, Table S2). The uncertainty in E_{LUC} accumulated to ±10 Pg C in cumulative E_{LUC} for 1750-2007. For vegetation and soil carbon the uncertainty introduced due to the choice of LUC reconstruction was ±13 and ±41 Pg C, respectively, in 1998-2007, translating into a change of each 3 % of the respective average size of vegetation and soil C stocks (Table 2, see Fig. S3 for regional differences for entire simulation

415   period). These uncertainties are higher for vegetation C stocks compared to the ones found by Arora and Boer (2010), and about the same size for those in soils found by the same study with only two of the LUC models applied here, implying non-linear interactions between DGVM structure and LUC dataset. We would expect uncertainty in C stocks and fluxes to increase, at least during the pre-1900 period, if also LUC reconstructions applying a non-linear development of per capita land use would be considered, such as for example the KK10

420   dataset does for the period 8 000 BC to AD 1850 (Kaplan et al., 2010).

For Europe the uncertainty in E_{LUC} is also large with ±37, ±33 and ±20 Tg C a^{-1} for the 1980s, 1990s and 2000s, which are between 30 % and 72 % of the average flux (Table 3). Differences result mainly from a disagreement in the amount of pastures between the LUC reconstructions, where the comparison is impaired by different definitions of the pasture class (see methods). This highlights the problem of fundamentally different structures

425   and assumptions between LUC models and DGVMs, recently being identified as a major uncertainty in model estimates of E_{LUC} (Pongratz et al., 2014). Although forests, natural grasslands and pastures can show similar gross primary productivity (GPP), they significantly vary in their C sequestration potential in vegetation and soils also depending on their location within Europe (Ciais et al., 2008; Schulze et al., 2010). For instance higher pasture areas in HILDA in southern Europe compared to LUH lead to an increase in vegetation C under LUC,

430   while a decrease was simulated with LUH (Fig. S4). The productivity and carbon dynamics of croplands in LPJ-GUESS is mainly governed by the crop selection, the bioclimatic conditions of the land where the crop is planted and the degree of fertilization and irrigation (for productivity of croplands under different degrees of fertilization see also Ciais et al., 2010; Schulze et al., 2010). For instance in Poland, high cropland fractions in LUH that were only marginally fertilized compared to croplands in western Europe, decreased NPP but

435   increased vegetation and soil C under LUC (Fig. S4). Differences between the LUC reconstructions and therefore uncertainties in C stocks and fluxes converge until the second half of the 19th century (maps not shown). Vegetation C stocks derived with HILDA are lower than estimates of Fuchs et al. (Fuchs et al., 2015a and personal communication) using the same datasets (minor difference in net data, see methods) and a

bookkeeping method but are within the uncertainty spanned by using HILDA and LUH net LUC datasets (Table
440   S3).

It is important to consider that the relative uncertainties in LUC transitions between datasets are not constant
through time, although the absolute uncertainties remain remarkably constant over the simulation period. The
relative deviation of pasture area for the three global datasets was about ±36 % before the 1850s, decreasing to
about ±10 % in the 2000s (Fig. S5c). Global cropland areas had a deviation of about ±13 % in the 1700,
445   decreasing to below ±2 % in the 2000s (Fig. S5c). For Europe the agreement of the two LUC reconstructions is
high for croplands (average deviation ±2 % for 1900-2010) but lower for pastures and natural areas (1900-2010
on average ±36 % for pastures and ±21 % for natural areas) with the deviation increasing until 2010 for pastures
(Fig. S5d). The general agreement on the fractional coverage of natural land, pastures and croplands is higher for
the periods after 1960, when FAO statistical data and later improved data from satellites became available (see
450   also Houghton, 2010; Verburg et al., 2011). Before this period, the extrapolation of historical LUC information
was very much dependent on the applied model algorithms in combination with census data. LUC
reconstructions also differ in the resolution of past LUC changes, providing annual time steps (RAMA for entire
historical period, LUH, HYDE after 2000) or originating from decadal aggregations (HILDA for entire historical
period, LUH, HYDE until 2000). Such methodological discrepancies and artifacts from the LUC modeling
455   significantly overlay the observed trends in the LUC reconstructions (compare Fig. 1c, d) and are included in
simulated C stocks and fluxes (Fig. 2, Fig. 3).

4.2.   Uncertainties in carbon stocks and fluxes due to accounting for gross land transitions

The consideration of detailed gross land conversions in our simulations increased the effects of LUC and
changes therein as larger areas were converted (Fig. 1c, d). The increase of about 16 % in average net annual
460   E_{LUC} and 15 % in cumulative E_{LUC} (Table 2, change due to gross relative to net, 1750-2014) compared well with
previous estimates (Table S4). The effect of shifting cultivation on cumulative E_{LUC} was quantified by Olofsson
and Hickler (2008) by using the LPJ model (Sitch et al., 2003), which has similarities in the way plant and soil
physiological processes are calculated to the model used here, but a simpler representation of vegetation
dynamics and croplands and no C-N dynamics. They found an increase in cumulative E_{LUC} by 28 % and 29 %
465   for 1700-1990 and 1850-1990, whilst Stocker et al. (2014), using a model with coupled C-N dynamics on 1x1°
spatial resolution, reported an increase by 15 %. The combined effect of shifting cultivation and wood harvest on
cumulative E_{LUC} was summarized by Houghton et al. (2012) as an increase by 25–35 %, and Wilkenskjeld et al.
(2014) found an increase in cumulative E_{LUC} of 61 % (51 % without the effect of wood harvest). Shevliakova et
al. (2013) provide an estimate of E_{LUC} under gross transitions including wood harvest for the period 1860-2005
470   using a combination of modeled C fluxes and a bookkeeping method to derive E_{LUC} that is fairly close to the
value calculated in this study. For total land C stocks Shevliakova et al. (2009) reported an additional loss of
49 % due to shifting cultivation and wood harvest and concluded from this that the effect on land carbon losses
was comparable in magnitude to the effect of cropland and pasture expansion. In our study we quantified an
additional loss of 39 % total C globally due to shifting cultivation alone in addition to net LUC (Table S4). Of
475   these studies, only the model of Stocker et al. (2014), to which our estimates are very similar (Table S4),
accounts for C-N interactions. C-N interactions have previously been found to enhance LUC emissions (Jain et
al., 2013). Apart from this all studies differ in the model type used, LUC data sets and climate model data
applied and the process representations in the models from the ones applied here. All studies except Olofsson
and Hickler (2008) applied spatial resolutions above the 0.5° applied here (1° or ~2°, see Table S4).

480   In the conducted global experiment the only contribution of gross land changes came from tropical shifting
cultivation, implemented in the LUH dataset based on assumed spatial extension and transition rates, reflected in
significantly increased rates of deforestation and reforestation in gross simulations (Fig. 4a). As would be
expected, the removal of forest material from the system through harvest or burning of cleared vegetation,
instead entering the soil pool through litter decomposition, reduces soil C content. However, the soil C losses are
485   much less marked than those in vegetation, perhaps reflecting a dominance of vegetation carbon turnover by
leaves and fine roots in LPJ-GUESS, inputs of C from which are less affected by harvesting of vegetation.

In comparison to the global gross land transitions that relied on a single process with uniform assumptions
regarding cultivation cycles, the European gross dataset accounted for irregular land changes based on regionally

available empirical evidence (national statistics and maps). E_{LUC} when accounting for gross land changes was
490 about 53 % higher in the first simulation decade and converged until minor differences from about 1980 on (Fig.
3a). Since LUC in Europe developed from being a source of C in the beginning of the 1900s to being a sink after
about 1960, the small difference in C stocks and fluxes when accounting for gross transitions in addition to net
land changes delayed the cumulated positive effects of the land changes. Thus the sink capacity of cumulative
E_{LUC} in the 2000s was reduced, as were increases in vegetation and soil C stocks (Fig. 3b, e, f). To our
495 knowledge no previous studies are available in which E_{LUC} for Europe was derived under net and gross LUC.
The effect of accounting for gross land transitions on vegetation C was negative in our simulations, with
vegetation C under gross LUC about 2 % lower than under net LUC, because the increased number of re-
growing stands under higher land transitions lowered mean forest canopy closure, which also lowered NPP and,
ultimately, soil C (see Table 3). In contrast Fuchs et al. (Fuchs et al., 2015a and unpublished results) using a
500 bookkeeping method derived about 1 % higher vegetation C stocks under gross LUC for the same area (Table
S3). Discrepancies result from major methodological differences between the bookkeeping and process-based
approach and also Fuchs et al. not accounting for C stocks in croplands and pastures.

Gross LUC transitions in Europe over the entire simulation period were dominated by conversions between
pastures and croplands, i.e. cropland or pasture expansion and cropland abandonment (Fig. 4b), that were direct
505 adjustments to market demands and changes in land-use related policies. Apart from this, LUC in Europe was
dominated by abandonment of agricultural land and reforestation peaking in the 1970s. Reforestation of
European grasslands was reported to entail a reduction in soil C stocks and an increase in vegetation C (Schulze
et al., 2010, Fig. 3e, f), and therefore a positive LUC flux (Fig. 3a). After a first period of regrowth, the
additional tree biomass and increased litter inputs to soils balanced soil C losses and vegetation and soil stocks
510 increased in the second half of the 19th century considering that wood harvest has been lower than growth (e.g.
Ciais et al., 2008), thereby contributing to the LUC sink capacity. Because land abandonment and reforestation
are one-directional LUC changes which are represented in the same way in net and gross HILDA data (see Fuchs
et al., 2015b), this did not lead to major differences between net and gross simulations. It has to be considered
that with its current four LUC classes, the LPJ-GUESS model was not able to make full use of the HILDA LUC
515 dataset, as not all HILDA land-cover classes were represented, e.g. urbanization (urban areas were assigned to
the barren LUC class, see methods), causing ~18 % of gross land changes between 1900-2010 (Fuchs et al.,
2015b).

4.3. Uncertainties in the modeling approach

The effects and uncertainties discussed here are to be seen relative to other uncertainties arising in the general
520 modeling process (e.g. different model implementations in respect to representation of LUC and changes therein,
treatment of environmental change). A meta-analysis by Houghton et al. (2012) estimated the uncertainty in
E_{LUC} arising from the applied modeling approach and method to be in the range of ±0.2 Pg C a[-1] and that due to
data-related uncertainty and incomplete process understanding to be in the range of ±0.5 Pg C a[-1], however, the
complex linkages between the contributing factors have made it difficult to attribute uncertainties to their sources
525 (see also Jain et al., 2013). Consideration of C-N interaction in vegetation and soils, as was done in this study, is
important when studying the effects of environmental drivers such as LUC on carbon emissions, however, with
the exception of a very few models (e.g. Jain et al., 2013; Smith et al., 2014; Xu-Ri and Prentice, 2008; Zaehle
and Friend, 2010), most models do not represent N cycling. We did not quantify the effect of C-N interactions in
this study, but we note that our estimates of cumulative E_{LUC} from 1850 to 2005 with net HYDE (Table S4) are
530 about 2 % lower than those of Pugh et al. (2015) using a version of LPJ-GUESS without C-N interactions. This
is in opposition to the findings of Jain et al. (2013) who found globally about 40 % higher E_{LUC} when accounting
for N dynamics and N limitation.

Implementation of gross transitions with the DGVM might be subject to considerable uncertainty. By adjusting
the minimum age upon which a regrowing natural stand becomes eligible for clearance again between 5 and 30
535 years (recalling that natural stands are removed in order of age when natural vegetation is reduced, see methods),
a deviation in cumulative E_{LUC} of ±20 Pg C (10 %) was found (1900-2014, LUH only, results not shown).
Underestimating this age would lead to considerable underestimates of E_{LUC} in our model structure, and this
highlights an important, and hitherto unremarked upon, implementation uncertainty for including gross

540 transitions in DGVM simulations. Wood harvest, which was not accounted for in this study, was assessed to account for an additional release of 0.2-0.3 Pg C a^{-1} mainly in extra-tropical regions (Houghton et al., 2012).

Simulation results of biogeochemical cycles with an LPJ-GUESS-type DGVM depend critically on the year when simulations are started, e.g. for LUH started in 1700 and 1900 (Fig. S6). For instance, E_{LUC} cumulated over 1950-2014 was 17 % and soil C was about 33 Pg C (2 %) lower when simulations were started in 1900 as opposed to 1700, while vegetation C stocks were similar (net LUC, Table S5). This emphasizes the impact of

545 legacy emissions of previous LUC changes on simulation results (see, e.g. Gasser and Ciais, 2013 for legacy fluxes and Pugh et al., 2015 for breakdown of LUC emissions). To exclude this effect from the analysis of uncertainties due to LUC dataset selection and the effect of accounting for gross LUC transitions, all global simulations were started in 1700. Likewise, simulations for Europe were started in 1900 for both HILDA and LUH to ensure comparability.

550

5. Conclusions

Global and European carbon stocks and fluxes and the effects of changes in LUC were shown to be subject to significant uncertainties resulting from the choice of historical LUC reconstruction. In our global simulations, HYDE and RAMA data often lead to similar results, while C stocks and fluxes predicted based on LUH data had

555 somewhat higher deviations from the 3-model mean. This is surprising considering the same data inputs and similar assumptions on land change trends and allocation of HYDE and LUH. For Europe, variables predicted based on the newly available HILDA dataset were similar to those resulting from using LUH for Europe, however LUH predicted larger changes under LUC. Differences in the effects of both global and European LUC on C stocks and fluxes were found to be mainly based on the total area and spatial distribution of pastures in the

560 datasets, although the area of pastures is impaired by different classifications used by the LUC models. To account for the uncertainty arising from different reconstructions of historical LUC in the dynamic modeling of C stocks and fluxes and to provide realistic estimates of this uncertainty for the land-use C flux, the consideration of multiple LUC reconstructions exploring the full range of reasonable assumptions is needed, as well as efforts to narrow the uncertainty in constructions of historical land-use. This goes along with the

565 reduction of uncertainties in the implementation of these datasets and different forms of LUC in DGVMs which has recently been the focus of discussion (Pongratz et al., 2014; Pugh et al., 2015; Stocker and Joos, 2015).

The results herein showed that considering gross land conversions significantly increased the effect of LUC change on C stocks and fluxes. Most noticeably the land-use C flux was enhanced by about 15 % of carbon released in addition to when only accounting for net land changes (cumulated 1750-2014), primarily resulting

570 from a reduction in vegetation C storage. Note that for DGVMs operating at a lower spatial resolution than the 0.5° x 0.5° used here, the underestimation of E_{LUC} would be even larger. Given the large percentage enhancements in E_{LUC} found by considering gross transitions, this should be the preferred method whenever possible.

Implementation of gross land-use transitions, however, poses technical and parameterization challenges to the

575 process-based models. It also relies on extensive information on historical land-use transitions, which is largely lacking; at present, only a few LUC models are able to represent gross land changes on larger spatial scales, providing a limited basis to characterize the uncertainty. The LUH dataset is the only global scale reconstruction representing gross land changes by explicitly implementing shifting cultivation in tropical areas with assuming a fixed period of 15 years for which land is cultivated before abandonment. For Europe, the HILDA data set is the

580 first reconstruction representing gross land transitions which are based on actual LUC inventory data and complementary model assumptions. The reconstruction of detailed regional sub-grid land transitions and possibly more realistic patterns of shifting cultivation today is restricted by the lack of reliable information on continental and global-scale historical land transitions. New datasets based on archived LUC data and remote sensing sources are currently becoming available with high spatial resolution for global to continental scale

585 (Chen et al., 2014; European Environment Agency, 2014; Wang et al., 2015) and on national to regional level (Homer et al., 2015; MOFOR, 2016; RCMRD, 2016; Roy et al., 2015; TerraClass, 2016). New promising efforts also provide LUC change data globally derived from remote sensing with 250m spatial resolution (Wang et al.,

2015) and with 30m spatial resolution (add the Globeland reference). In the coming years new high resolution
LUC data set can be expected from the Landsat archives (http://earthexplorer.usgs.gov) and the new Sentinel
590 missions (Aschbacher and Milagro-Pérez, 2012). These will contribute to close the information gap and with this
improve the calibration of LUC models to represent the underlying processes, reduce the uncertainty in
ecosystem functions such as the present-day land-use flux, and provide enhanced information for example for
the assessment of ecosystem services and biodiversity indicators in the future.

595   **Acknowledgements**

This work was funded by the European Commission's 7th Framework Program under Grant Agreement numbers
308393 (OPERAs) and 603542 (LUC4C). This work was supported, in part, by the German Federal Ministry of
Education and Research (BMBF), through the Helmholtz Association and its research program ATMO. The
authors thank Stefan Olin from Lund University for advice on C-N cycling in crops.

600

Author contributions

AB, TP and AA conceived and designed the experiments. ML realized the technical implementation of gross
land changes in LPJ-GUESS. AB carried out the model simulations and led the data analysis, with contributions
from all authors. RF contributed the HILDA land-use data. AB led the writing of the manuscript with
605   contributions from all authors.

References

Ahlström, A., Schurgers, G., Arneth, A. and Smith, B.: Robustness and uncertainty in terrestrial ecosystem
carbon response to CMIP5 climate change projections, Environ. Res. Lett., 7(4), 9 p., doi:10.1088/1748-
610   9326/7/4/044008, 2012.

Arora, V. K. and Boer, G. J.: Uncertainties in the 20th century carbon budget associated with land use change,
Glob. Chang. Biol., 16(12), 3327–3348, doi:10.1111/j.1365-2486.2010.02202.x, 2010.

Aschbacher, J. and Milagro-Pérez, M. P.: The European Earth monitoring (GMES) programme: Status and
perspectives, Remote Sens. Environ., 120(2012), 3–8, doi:10.1016/j.rse.2011.08.028, 2012.

615   van Asselen, S. and Verburg, P. H.: Land cover change or land-use intensification: simulating land system
change with a global-scale land change model., Glob. Chang. Biol., 19(12), 3648–67, doi:10.1111/gcb.12331,
2013.

Baccini, A., Goetz, S. J., Walker, W. S., Laporte, N. T., Sun, M., Sulla-Menashe, D., Hackler, J., Beck, P. S. A.,
Dubayah, R., Friedl, M. A., Samanta, S. and Houghton, R. A.: Estimated carbon dioxide emissions from tropical
620   deforestation improved by carbon-density maps, Nat. Clim. Chang., 2(3), 182–185, doi:10.1038/nclimate1354,
2012.

Bugmann, H.: A review of forest gap models, Clim. Change, 51, 259–305, 2001.

Chen, J., Chen, J., Liao, A., Cao, X., Chen, L., Chen, X., He, C., Han, G., Peng, S., Lu, M., Zhang, W., Tong, X.
and Mills, J.: Global land cover mapping at 30m resolution: A POK-based operational approach, ISPRS J.
625   Photogramm. Remote Sens., 103, 7–27, doi:10.1016/j.isprsjprs.2014.09.002, 2014.

Ciais, P., Schelhaas, M. J., Zaehle, S., Piao, S. L., Cescatti, A., Liski, J., Luyssaert, S., Le-Maire, G., Schulze, E.-
D., Bouriaud, O., Freibauer, A., Valentini, R. and Nabuurs, G. J.: Carbon accumulation in European forests, Nat.
Geosci., 1(7), 425–429, doi:10.1038/ngeo233, 2008.

Ciais, P., Wattenbach, M., Vuichard, N., Smith, P., Piao, S. L., Don, A., Luyssaert, S., Janssens, I. A., Bondeau,
630   A., Dechow, R., Leip, A., Smith, P. C., Beer, C., Van der Werf, G. R., Gervois, S., Van Oost, K., Tomelleri, E.,
Freibauer, A. and Schulze, E. D.: The European carbon balance. Part 2: Croplands, Glob. Chang. Biol., 16(5),
1409–1428, doi:10.1111/j.1365-2486.2009.02055.x, 2010.

deB Richter, D. and Houghton, R.: Fluxes From Land-Use Change: Implications for Reducing Global Emissions
and Increasing Sinks, Carbon Manag., 2(1), 41–47, doi:10.4155/cmt.10.43, 2011.

635   European Environment Agency: CLC2012. Addendum to CLC2006 Technical Guidelines., 2014.

Fuchs, R., Herold, M., Verburg, P. H. and Clevers, J. G. P. W.: A high-resolution and harmonized model approach for reconstructing and analysing historic land changes in Europe, Biogeosciences, 10(3), 1543–1559, doi:10.5194/bg-10-1543-2013, 2013.

Fuchs, R., Schulp, C. J. E., Hengeveld, G. M., Verburg, P. H., Clevers, J. G. P. W., Schelhaas, M.-J. and Herold, 640   M.: Assessing the influence of historic net and gross land changes on the carbon fluxes of Europe, Glob. Chang. Biol., (March 2016), 1–14, doi:10.1111/gcb.13191, 2015a.

Fuchs, R., Herold, M., Verburg, P. H., Clevers, J. G. P. W. and Eberle, J.: Gross changes in reconstructions of historic land cover/use for Europe between 1900 and 2010., Glob. Chang. Biol. Biol., 21, 299–313, doi:10.1111/gcb.12714, 2015b.

645   Fuchs, R., Verburg, P. H., Clevers, J. G. P. W. and Herold, M.: The potential of old maps and encyclopaedias for reconstructing historic European land cover/use change, Appl. Geogr., 59(March 2016), 43–55, doi:10.1016/j.apgeog.2015.02.013, 2015c.

Gasser, T. and Ciais, P.: A theoretical framework for the net land-to-atmosphere CO_2 flux and its implications in the definition of "emissions from land-use change," Earth Syst. Dyn., 4(1), 171–186, doi:10.5194/esd-4-171-650   2013, 2013.

Guo, L. B. and Gifford, R. M.: Soil carbon stocks and land use change: A meta analysis, Glob. Chang. Biol., 8(4), 345–360, doi:10.1046/j.1354-1013.2002.00486.x, 2002.

Hickler, T., Smith, B., Sykes, M. T., Davis, M. B., Walker, K. and Sugita, S.: Using a Generalized Vegetation Model to Simulate Vegetation Dynamics in Northeastern USA, Ecology, 85(2), 519–530, 2004.

655   Hickler, T., Prentice, I. C., Smith, B. and Sykes, M. T.: Implementing plant hydraulic architecture within the LPJ Dynamic Global Vegetation Model, , 567–577, doi:10.1111/j.1466-822x.2006.00254.x, 2006.

Hickler, T., Vohland, K., Feehan, J., Miller, P. A., Smith, B., Costa, L., Giesecke, T., Fronzek, S., Carter, T. R., Cramer, W., Kuehn, I. and Sykes, M. T.: Projecting the future distribution of European potential natural vegetation zones with a generalized, tree species-based dynamic vegetation model, Glob. Ecol. Biogeogr., 21, 660   50–63, 2012.

Homer, C. G., Dewitz, J. A., Yang, L., Jin, S., Danielson, P., Xian, G., Coulston, J., Herold, N. D., Wickham, J. D. and Megown, K.: Completion of the 2011 National Land Cover Database for the conterminous United States-Representing a decade of land cover change information, Photogramm. Eng. Remote Sensing, 81(5), 345–354, doi:10.14358/PERS.81.5.345, 2015.

665   Houghton, R. A.: Carbon Flux to the Atmosphere from Land-Use Changes: 1850-2005, in TRENDS: A Compendium of Data on Global Change, Carbon Dioxide Information Analysis Center, Oak Ridge National Laboratory, U.S. Department of Energy, Oak Ridge, Tenn., U.S.A., 2008.

Houghton, R. A.: How well do we know the flux of CO_2 from land-use change?, Tellus, Ser. B Chem. Phys. Meteorol., 62(5), 337–351, doi:10.1111/j.1600-0889.2010.00473.x, 2010.

670   Houghton, R. A., House, J. I., Pongratz, J., van der Werf, G. R., DeFries, R. S., Hansen, M. C., Le Quéré, C. and Ramankutty, N.: Carbon emissions from land use and land-cover change, Biogeosciences, 9(12), 5125–5142, doi:10.5194/bg-9-5125-2012, 2012.

Hurtt, G. C., Chini, L. P., Frolking, S., Betts, R. A., Feddema, J., Fischer, G., Fisk, J. P., Hibbard, K., Houghton, R. A., Janetos, A., Jones, C. D., Kindermann, G., Kinoshita, T., Klein Goldewijk, K., Riahi, K., Shevliakova, E., 675   Smith, S., Stehfest, E., Thomson, A., Thornton, P., van Vuuren, D. P. and Wang, Y. P.: Harmonization of land-use scenarios for the period 1500–2100: 600 years of global gridded annual land-use transitions, wood harvest, and resulting secondary lands, Clim. Change, 109, 117–161, 2011.

Jain, A. K., Meiyappan, P., Song, Y. and House, J. I.: CO 2 emissions from land-use change affected more by nitrogen cycle, than by the choice of land-cover data, Glob. Chang. Biol., 19(9), 2893–2906, 680   doi:10.1111/gcb.12207, 2013.

Kaplan, J. O., Krumhardt, K. M. and Zimmermann, N.: The prehistoric and preindustrial deforestation of Europe, Quat. Sci. Rev., 28(27-28), 3016–3034, doi:10.1016/j.quascirev.2009.09.028, 2009.

Kaplan, J. O., Krumhardt, K. M., Ellis, E. C., Ruddiman, W. F., Lemmen, C. and Goldewijk, K. K.: Holocene carbon emissions as a result of anthropogenic land cover change, The Holocene, 21(5), 775–791, 685   doi:10.1177/0959683610386983, 2010.

Kaplan, J. O., Krumhardt, K. M. and Zimmermann, N. E.: The effects of land use and climate change on the carbon cycle of Europe over the past 500 years, Glob. Chang. Biol., 18(3), 902–914, doi:10.1111/j.1365-2486.2011.02580.x, 2012.

690   Klein Goldewijk, K. and Verburg, P. H.: Uncertainties in global-scale reconstructions of historical land use: an illustration using the HYDE data set, Landsc. Ecol., 28(5), 861–877, doi:10.1007/s10980-013-9877-x, 2013.

Klein Goldewijk, K., Beusen, A. and Janssen, P.: Long-term dynamic modeling of global population and built-up area in a spatially explicit way: HYDE 3.1, The Holocene, 20(4), 565–573, doi:10.1177/0959683609356587, 2010.

Klein Goldewijk, K., Beusen, A., Van Drecht, G. and De Vos, M.: The HYDE 3.1 spatially explicit database of
695   human-induced global land-use change over the past 12,000 years, Glob. Ecol. Biogeogr., 20(1), 73–86, doi:10.1111/j.1466-8238.2010.00587.x, 2011.

Krause, A., Pugh, T. A. M., Bayer, A. D., Lindeskog, M. and Arneth, A.: Impacts of land-use history on the recovery of ecosystems after agricultural abandonment, Earth Syst. Dyn. Discuss., (April), 1–38, doi:10.5194/esd-2016-11, 2016.

700   Lamarque, J. F., Bond, T. C., Eyring, V., Granier, C., Heil, A., Klimont, Z., Lee, D., Liousse, C., Mieville, A., Owen, B., Schultz, M. G., Shindell, D., Smith, S. J., Stehfest, E., Van Aardenne, J., Cooper, O. R., Kainuma, M., Mahowald, N., McConnell, J. R., Naik, V., Riahi, K. and Van Vuuren, D. P.: Historical (1850-2000) gridded anthropogenic and biomass burning emissions of reactive gases and aerosols: Methodology and application, Atmos. Chem. Phys., 10(15), 7017–7039, doi:10.5194/acp-10-7017-2010, 2010.

705   Lamarque, J.-F., Kyle, G. P., Meinshausen, M., Riahi, K., Smith, S. J., van Vuuren, D. P., Conley, A. J. and Vitt, F.: Global and regional evolution of short-lived radiatively-active gases and aerosols in the Representative Concentration Pathways, Clim. Change, 109(1-2), 191–212, doi:10.1007/s10584-011-0155-0, 2011.

Lindeskog, M., Arneth, A., Bondeau, A., Waha, K., Seaquist, J., Olin, S. and Smith, B.: Implications of accounting for land use in simulations of ecosystem carbon cycling in Africa, Earth Syst. Dyn., 4(2), 385–407,
710   doi:10.5194/esd-4-385-2013, 2013.

McGuire, A. D., Sitch, S., Clein, J. S., Dargaville, R., Esser, G., Foley, J., Heimann, M., Joos, F., Kaplan, J., Kicklighter, D. W., Meier, R. A., Melillo, J. M., Moore B. III, Prentice, I. C., Ramankutty, N., Reichenau, T., Schloss, A., Tian, H., Williams, L. J. and Wittenberg, U.: Carbon balance of the terrestrial biosphere in the twentieth century: analyses of CO2, climate and land use effects with four process-based models, Global
715   Biogeochem. Cycles, 15(1), 183–206, doi:Doi 10.1029/2000gb001298, 2001.

McLauchlan, K.: The nature and longevity of agricultural impacts on soil carbon and nutrients: A review, Ecosystems, 9(8), 1364–1382, doi:10.1007/s10021-005-0135-1, 2006.

MOFOR: Land use data for Indonesia, [online] Available from: http://webgis.dephut.go.id:8080/kemenhut/index.php/en/, 2016.

720   Morales, P., Sykes, M. T., Prentice, I. C., Smith, P., Smith, B., Bugmann, H., Zierl, B., Friedlingstein, P., Viovy, N., Sabate, S., Sanchez, A., Pla, E., Gracia, C. A., Sitch, S., Arneth, A. and Ogee, J.: Comparing and evaluating process-based ecosystem model predictions of carbon and water fluxes in major European forest biomes, Glob. Chang. Biol., 11 , 2211–2233, 2005.

Olin, S., Schurgers, G., Lindeskog, M., Wårlind, D., Smith, B., Bodin, P., Holmér, J. and Arneth, A.: Modelling
725   the response of yields and tissue C N to changes in atmospheric CO2 and N management in the main wheat regions of western Europe, Biogeosciences, 12(8), 2489–2515, doi:10.5194/bg-12-2489-2015, 2015.

Olofsson, J. and Hickler, T.: Effects of human land-use on the global carbon cycle during the last 6,000 years, Veget Hist Archaeobot, 17, 605–615, 2008.

Piao, S., Sitch, S., Ciais, P., Friedlingstein, P., Peylin, P., Wang, X., Ahlström, A., Anav, A., Canadell, J. G.,
730   Cong, N., Huntingford, C., Jung, M., Levis, S., Levy, P. E., J., L., Lin, X., Lomas, M. R., Lu, M., Luo, Y., Ma, Y., Myneni, R. B., Poulter, B., Sun, Z., Wang, T., Viovy, N., Zaehle, S. and Zeng, N.: Evaluation of terrestrial carbon cycle models for their response to climate variability and to CO2 trends, Glob. Chang. Biol., 19, 2117–2132, 2013.

Pongratz, J., Reick, C., Raddatz, T. and Claussen, M.: A reconstruction of global agricultural areas and land
735   cover for the last millennium, Global Biogeochem. Cycles, 22(3), doi:10.1029/2007GB003153, 2008.

Pongratz, J., Reick, C. H., Raddatz, T. and Claussen, M.: Biogeophysical versus biogeochemical climate response to historical anthropogenic land cover change, Geophys. Res. Lett., 37(8), 1–5, doi:10.1029/2010GL043010, 2010.

Pongratz, J., Reick, C. H., Houghton, R. A. and House, J. I.: Terminology as a key uncertainty in net land use
740   and land cover change carbon flux estimates, Earth Syst. Dyn., 5(1), 177–195, doi:10.5194/esd-5-177-2014, 2014.

Portmann, F. T., Siebert, S. and Döll, P.: MIRCA2000-Global monthly irrigated and rainfed crop areas around

the year 2000: A new high-resolution data set for agricultural and hydrological modeling, Global Biogeochem. Cycles, 24(1), 1–24, doi:10.1029/2008GB003435, 2010.

745   Pugh, T. A. M., Arneth, A., Olin, S., Ahlström, A., Bayer, A. D., Goldewijk, K. K., Lindeskog, M. and Schurgers, G.: Simulated carbon emissions from land-use change are substantially enhanced by accounting for agricultural management, Environ. Res. Lett., 10(12), 124008, doi:10.1088/1748-9326/10/12/124008, 2015.

        Le Quéré, C., Peters, G. P., Andres, R. J., Andrew, R. M., Boden, T., Ciais, P., Friedlingstein, P., Houghton, R. A., Marland, G., Moriarty, R., Sitch, S., Trans, P., Arneth, A., Arvanitis, A., E, B. D. C., Bopp, L., Canadell, J.
750   G., Chini, L. P., Doney, S. C., Harper, A., Harris, I., House, J. I., Jain, A. K., Jones, S. D., E, K., Keeling, R. F., Klein Goldewijk, K., Körtzinger, A., Koven, C., Lefevre, N., Omar, A., Ono, T., Park, G.-H. G.-H., Pfeil, B., Poulter, B., Raupach, M. R., Regnier, P., Rödenbeck, C., Saito, S., Schwinger, J., Stocker, B. D., Tilbrook, B., van Heuven, S., Viovy, N., Wanninkhof, R., Wiltshire, A., Zaehle, S., Yue, C., Tans, P., Arneth, A., Arvanitis, A., Bakker, D. C. E., Bopp, L., Canadell, J. G., Chini, L. P., Doney, S. C., Harper, A., Harris, I., House, J. I.,
755   Jain, A. K., Jones, S. D., Kato, E., Keeling, R. F., Klein Goldewijk, K., Körtzinger, A., Koven, C., Lefèvre, N., Omar, A., Ono, T., Park, G.-H. G.-H., Pfeil, B., Poulter, B., Raupach, M. R., Regnier, P., Rödenbeck, C., Saito, S., Schwinger, J., Stocker, B. D., Tilbrook, B., van Heuven, S., Viovy, N., Wanninkhof, R., Wiltshire, A., Zaehle, S. and Yue, C.: Global carbon budget 2013, Earth Syst. Sci. Data Discuss., 6 (2), 689–760, doi:10.5194/essdd-6-689-2013, 2013.

760   Le Quéré, C., Moriarty, R., Andrew, R. M., Peters, G. P., Ciais, P., Friedlingstein, P., Jones, S. D., Sitch, S., Tans, P., Arneth, A., Boden, T. a., Bopp, L., Bozec, Y., Canadell, J. G., Chini, L. P., Chevallier, F., Cosca, C. E., Harris, I., Hoppema, M., Houghton, R. a., House, J. I., Jain, a. K., Johannessen, T., Kato, E., Keeling, R. F., Kitidis, V., Klein Goldewijk, K., Koven, C., Landa, C. S., Landschützer, P., Lenton, A., Lima, I. D., Marland, G., Mathis, J. T., Metzl, N., Nojiri, Y., Olsen, A., Ono, T., Peng, S., Peters, W., Pfeil, B., Poulter, B., Raupach,
765   M. R., Regnier, P., Rödenbeck, C., Saito, S., Salisbury, J. E., Schuster, U., Schwinger, J., Séférian, R., Segschneider, J., Steinhoff, T., Stocker, B. D., Sutton, a. J., Takahashi, T., Tilbrook, B., van der Werf, G. R., Viovy, N., Wang, Y.-P., Wanninkhof, R., Wiltshire, A. and Zeng, N.: Global carbon budget 2014, Earth Syst. Sci. Data, 7(1), 47–85, doi:10.5194/essd-7-47-2015, 2015.

        Ramankutty, N.: Global Cropland and Pasture Data from 1700–2007, [online] Available from:
770   http://www.geog.mcgill.ca/nramankutty/Datasets/Datasets.html, 2012.

        Ramankutty, N. and Foley, J. A.: Estimating historical changes in global land cover: Croplands from 1700 to 1992, Global Biogeochem. Cycles, 13(4), 997–1027, doi:10.1029/2009GB003765, 1999.

        RCMRD: Land-Cover Mapping for Greenhouse Gas Emissions Inventory in Africa, [online] Available from: http://www.servircatalogue.net/Product?product_id=18, 2016.

775   Roy, P. S., Roy, A., Joshi, P. K., Kale, M. P., Srivastava, V. K., Srivastava, S. K., Dwevidi, R. S., Joshi, C., Behera, M. D., Meiyappan, P., Sharma, Y., Jain, A. K., Singh, J. S., Palchowdhuri, Y., Ramachandran, R. M., Pinjarla, B., Chakravarthi, V., Babu, N., Gowsalya, M. S., Thiruvengadam, P., Kotteeswaran, M., Priya, V., Yelishetty, K. M. V. N., Maithani, S., Talukdar, G., Mondal, I., Rajan, K. S., Narendra, P. S., Biswal, S., Chakraborty, A., Padalia, H., Chavan, M., Pardeshi, S. N., Chaudhari, S. A., Anand, A., Vyas, A., Reddy, M. K.,
780   Ramalingam, M., Manonmani, R., Behera, P., Das, P., Tripathi, P., Matin, S., Khan, M. L., Tripathi, O. P., Deka, J., Kumar, P. and Kushwaha, D.: Development of decadal (1985-1995-2005) land use and land cover database for India, Remote Sens., 7(3), 2401–2430, doi:10.3390/rs70302401, 2015.

        Schulze, E. D., Ciais, P., Luyssaert, S., Schrumpf, M., Janssens, I. A., Thiruchittampalam, B., Theloke, J., Saurat, M., Bringezu, S., Lelieveld, J., Lohila, A., Rebmann, C., Jung, M., Bastviken, D., Abril, G., Grassi, G.,
785   Leip, A., Freibauer, A., Kutsch, W., Don, A., Nieschulze, J., Boerner, A., Gash, J. H. and Dolman, A. J.: The European carbon balance. Part 4: Integration of carbon and other trace-gas fluxes, Glob. Chang. Biol., 16(5), 1451–1469, doi:10.1111/j.1365-2486.2010.02215.x, 2010.

        Shevliakova, E., Pacala, S. W., Malyshev, S., Hurtt, G. C., Milly, P. C. D., Caspersen, J. P., Sentman, L. T., Fisk, J. P., Wirth, C. and Crevoisier, C.: Carbon cycling under 300 years of land use change: Importance of the
790   secondary vegetation sink, Global Biogeochem. Cycles, 23(2), 1–16, doi:10.1029/2007GB003176, 2009.

        Shevliakova, E., Stouffer, R. J., Malyshev, S., Krasting, J. P., Hurtt, G. C. and Pacala, S. W.: Historical warming reduced due to enhanced land carbon uptake., Proc. Natl. Acad. Sci. U. S. A., 110(42), 16730–5, doi:10.1073/pnas.1314047110, 2013.

        Sitch, S., Smith, B., Prentice, I. C., Arneth, A., Bondeau, A., Cramer, W., Kaplan, J. O., Levis, S., Lucht, W.,
795   Sykes, M. T., Thonicke, K. and Venevsky, S.: Evaluation of ecosystem dynamics, plant geography and terrestrial carbon cycling in the LPJ dynamic global vegetation model, Glob. Chang. Biol., 9, 161–185, 2003.

        Sitch, S., Friedlingstein, P., Gruber, N., Jones, S. D., Murray-Tortarolo, G., Ahlström, A., Doney, S. C., Graven, H., Heinze, C., Huntingford, C., Levis, S., Levy, P. E., Lomas, M., Poulter, B., Viovy, N., Zaehle, S., Zeng, N.,

800 Arneth, A., Bonan, G., Bopp, L., Canadell, J. G., Chevallier, F., Ciais, P., Ellis, R., Gloor, M., Peylin, P., Piao, S. L., Le Quéré, C., Smith, B., Zhu, Z. and Myneni, R.: Recent trends and drivers of regional sources and sinks of carbon dioxide, Biogeosciences, 12(3), 653–679, doi:10.5194/bg-12-653-2015, 2015.

Smith, B., Prentice, I. C. and Sykes, M. T.: Representation of vegetation dynamics in the modelling of terrestrial ecosystems: comparing two contrasting approaches within European climate space, Glob. Ecol. & Biogeogr. 10, 621– 637, 10, 621–637, 2001.

805 Smith, B., Wårlind, D., Arneth, A., Hickler, T., Leadley, P., Siltberg, J. and Zaehle, S.: Implications of incorporating N cycling and N limitations on primary production in an individual-based dynamic vegetation model, Biogeosciences Discuss., 11, 2017–2054, doi:10.5194/bgd-10-18613-2013, 2014.

Stocker, B. D. and Joos, F.: Quantifying differences in land use emission estimates implied by definition discrepancies, Earth Syst. Dyn., 6(2), 731–744, doi:10.5194/esd-6-731-2015, 2015.

810 Stocker, B. D., Feissli, F., Strssmann, K. M., Spahni, R., Joos, F. and Strassmann, K.: Past and future carbon fluxes from land use change, shifting cultivation and wood harvest, Tellus B, 1, 1–15, doi:10.3402/tellusb.v66.23188, 2014.

Tans, P. and Keeling, R.: Trends in atmospheric carbon dioxide, 2015.

TerraClass: Land use data for Brazilian Amazon region, [online] Available from:
815 http://www.inpe.br/cra/ingles/project_research/terraclass.php, 2016.

University of East Anglia Climatic Research Unit (CRU): CRU TS3.21: Climatic Research Unit (CRU) Time-Series (TS) Version 3.21 of High Resolution Gridded Data of Month-by-month Variation in Climate (Jan. 1901 - Dec. 2012), NCAS Br. Atmos. Data Centre, 2013, (March 2014), doi:10.5285/D0E1585D-3417-485F-87AE-4FCECF10A992, 2013.

820 Verburg, P. H., Neumann, K. and Nol, L.: Challenges in using land use and land cover data for global change studies, Glob. Chang. Biol., 17, 974–989, doi:10.1111/j.1365-2486.2010.02307.x, 2011.

Wang, J., Zhao, Y., Li, C., Yu, L., Liu, D. and Gong, P.: Mapping global land cover in 2001 and 2010 with spatial-temporal consistency at 250m resolution, ISPRS J. Photogramm. Remote Sens., 103, 38–47, doi:10.1016/j.isprsjprs.2014.03.007, 2015.

825 Wilkenskjeld, S., Kloster, S., Pongratz, J., Raddatz, T. and Reick, C.: Comparing the influence of net and gross anthropogenic land use and land cover changes on the carbon cycle in the MPI-ESM, Biogeosciences Discuss., 11(4), 5443–5469, doi:10.5194/bgd-11-5443-2014, 2014.

Wilkins, R. J., Hopkins, A. and Hatch, D. J.: Grassland in Europe, Grassl. Sci., 49, 258–266, 2003.

Williams, M.: Dark ages and dark areas: global deforestation in the deep past, J. Hist. Geogr., 26(1), 28–46,
830 doi:10.1006/jhge.1999.0189, 2000.

Xu-Ri and Prentice, I. C.: Terrestrial nitrogen cycle simulation with a dynamic global vegetation model, Glob. Chang. Biol., 14(8), 1745–1764, doi:10.1111/j.1365-2486.2008.01625.x, 2008.

Zaehle, S.: Terrestrial nitrogen-carbon cycle interactions at the global scale, Philos Trans R Soc L. B Biol Sci, 368(1621), 20130125, doi:10.1098/rstb.2013.0125, 2013.

835 Zaehle, S. and Friend, A. D.: Carbon and nitrogen cycle dynamics in the O-CN land surface model: 1. Model description, site-scale evaluation, and sensitivity to parameter estimates, Global Biogeochem. Cycles, 24(1), 1–13, doi:10.1029/2009GB003521, 2010.

Zaehle, S., Ciais, P., Friend, A. D. and Prieur, V.: Carbon benefits of anthropogenic reactive nitrogen offset by nitrous oxide emissions, Nat. Geosci., 4(9), 601–605, doi:10.1038/ngeo1207, 2011.

840

Table 1. Overview of LPJ-GUESS simulations carried out as part of this study.

Land-use model		First year	Last year	Representation of LUC transitions	Spatial coverage
Abbreviation	Reference				
LUH	1500-2005: Hurtt et al. (2011), extension until 2014: e.g. Le Quéré et al. (2015)	1700[a]	2014	gross	Globe
		1700[a]	2014	net	Globe
		1700[a]	2014	LUC fixed to 1700	Globe
HYDE	10 000 BC to AD 2000: Klein Goldewijk et al. (2011), extension until 2013: Klein Goldewijk et al. (2015), Le Quéré et al. (2015)	1700[a]	2013	net	Globe
		1700[a]	2013	LUC fixed to 1700	Globe
RAMA	1700-1992: Ramankutty and Foley (1999) extension until 2007: Ramankutty (2012)	1700	2007	net	Globe
		1700	2007	LUC fixed to 1700	Globe
HILDA	Fuchs et al. (2015b)	1900	2010	gross	EU27[b]+CH
		1900	2010	net	EU27[b]+CH
		1900	2010	LUC fixed to 1900	EU27[b]+CH
LUH	1500-2005: Hurtt et al. (2011) extension until 2014: e.g. Le Quéré et al. (2015)	1900[c]	2014	net	EU27[b]+CH
		1900[c]	2014	LUC fixed to 1900	EU27[b]+CH

[a]1700 was selected as earliest start year, [b]EU 2007-2013, [c]1900 was selected as start year for European simulations.

Earth System Dynamics — Discussions — Open Access

845 Table 2. Changes in C stocks and fluxes in global reconstructions of net and gross LUC changes. Land use change flux (E_{LUC}) and cumulative land use flux E_{LUC}, Net primary productivity (NPP), C stocks in vegetation and soils. Values are always given as 10-year averages (except LUC areas and cumulative flux).

	Averaging period	Calculation	Unit	LUH (net)	RAMA (net)	HYDE (net)	Average and uncertainty for the LUC models	LUH (gross)	difference LUH (gross-net)
Natural area	1700	A_{nat}	10^6 km^2	122.48	124.35	126.54	124.46 ± 2.03	122.48	0
Natural area	2007	A_{nat}	10^6 km^2	85.39	90.31	84.97	86.89 ± 2.97	85.39	0
Pasture area	1700	A_{pas}	10^6 km^2	7.45	4.89	3.32	5.22 ± 2.08	7.45	0
Pasture area	2007	A_{pas}	10^6 km^2	32.38	27.04	32.81	30.74 ± 3.21	32.38	0
Cropland area	1700	A_{crop}	10^6 km^2	2.80	3.49	2.86	3.05 ± 0.38	2.80	0
Cropland area	2007	A_{crop}	10^6 km^2	14.96	15.38	14.95	15.10 ± 0.25	14.96	0
Change in natural area	1700-2007	A_{nat}	10^6 km^2	-37.09	-34.04	-41.57	-37.57 ± 3.79	-37.09	0
Change in pasture area	1700-2007	A_{pas}	10^6 km^2	+24.93	+22.15	+29.49	+25.52 ± 3.71	+24.93	0
Change in cropland area	1700-2007	A_{crop}	10^6 km^2	+12.16	+11.89	+12.09	+12.05 ± 0.14	+12.16	0
Total area under transition	1700-2007	ΣA_{trans}	10^6 km^2	51.92	78.59	64.62	65.0 ± 13.3	243.80	+191.88
Change in area under transition	1850-1960	deltaA_{trans}	km^2 a^{-1}	+5137	+7259	+6703	+6366 ± 1101	+5549	+412
E_{LUC}	1750-2007	$E_{LUC\ Net/Gross}$	Pg C a^{-1}	0.81	0.87	0.89	0.86 ± 0.04	0.94	+0.13
E_{LUC}	1750-2014	$E_{LUC\ Net/Gross}$	Pg C a^{-1}	0.84	-	-	-	0.96	+0.12
E_{LUC}	1980-1989	$E_{LUC\ Net/Gross}$	Pg C a^{-1}	1.10	1.40	1.55	1.35 ± 0.23	1.28	+0.18
E_{LUC}	1990-1999	$E_{LUC\ Net/Gross}$	Pg C a^{-1}	1.18	1.57	2.65	1.80 ± 0.76	1.41	+0.23
E_{LUC}	1998-2007	$E_{LUC\ Net/Gross}$	Pg C a^{-1}	1.17	2.00	2.06	1.74 ± 0.49	1.38	+0.20
E_{LUC}	2005-2014	$E_{LUC\ Net/Gross}$	Pg C a^{-1}	1.50	-	-	-	1.64	+0.14
Cumulative E_{LUC}	1750-2007	$\Sigma E_{LUC\ Net/Gross}$	Pg C	210.02	225.18	228.95	221.38 ± 10.02	242.04	+32.02
Cumulative E_{LUC}	1750-2014	$\Sigma E_{LUC\ Net/Gross}$	Pg C	222.29	-	-	-	255.27	+32.98
NPP	1700-1709	$NPP_{Net/Gross}$	Pg C a^{-1}	50.18	52.10	52.21	51.50 ± 1.14	50.04	-0.14
NPP	1998-2007	$NPP_{Net/Gross}$	Pg C a^{-1}	58.9	59.79	60.85	59.85 ± 0.97	57.49	-1.42
NPP	2005-2014	$NPP_{Net/Gross}$	Pg C a^{-1}	59.95	-	-	-	58.46	-1.49
Change in NPP due to LUC	1998-2007	$NPP_{Net/Gross}$-NPP_{Ref}	Pg C a^{-1}	-1.92	-3.32	-2.44	-2.56 ± 0.71	-3.33	-1.42
Change in NPP due to LUC	2005-2014	$NPP_{Net/Gross}$-NPP_{Ref}	Pg C a^{-1}	-2.26	-	-	-	-3.75	-1.49
Vegetation C	1700-2014	$VegC_{Net/Gross}$	Pg C	435	-	-	-	419	-16
Vegetation C	1700-1709	$VegC_{Net/Gross}$	Pg C	464.18	495.70	497.19	485.69 ± 18.65	461.35	-2.83
Vegetation C	1998-2007	$VegC_{Net/Gross}$	Pg C	414.62	439.10	435.22	429.65 ± 13.15	380.43	-34.20
Vegetation C	2005-2014	$VegC_{Net/Gross}$	Pg C	421.48	-	-	-	386.64	-34.84
Change in vegetation C due to LUC	1960-1969	$VegC_{Net/Gross}$-$VegC_{Ref}$	Pg C	-109.49	-114.12	-108.21	-110.61 ± 3.11	-137.06	-27.58
Change in vegetation C due to LUC	1998-2007	$VegC_{Net/Gross}$-$VegC_{Ref}$	Pg C	-140.36	-153.41	-159.42	-151.06 ± 9.74	-174.56	-34.20
Change in vegetation C due to LUC	2005-2014	$VegC_{Net/Gross}$-$VegC_{Ref}$	Pg C	-148.43	-	-	-	-183.27	-34.27
Soil C	1700-2014	$SoilC_{Net/Gross}$	Pg C	1425.85	-	-	-	1420.81	-5.04
Soil C	1700-1709	$SoilC_{Net/Gross}$	Pg C	1445.96	1511.65	1516.06	1491.22 ± 39.26	1445.58	-0.38
Soil C	1998-2007	$SoilC_{Net/Gross}$	Pg C	1404.20	1471.83	1478.08	1451.37 ± 40.97	1393.43	-10.77
Soil C	2005-2014	$SoilC_{Net/Gross}$	Pg C	1406.78	-	-	-	1395.56	-11.22
Change in soil C due to LUC	1998-2007	$SoilC_{Net/Gross}$-$SoilC_{Ref}$	Pg C	-75.80	-75.04	-73.54	-74.79 ± 1.15	-86.57	-10.77
Change in soil C due to LUC	2005-2014	$SoilC_{Net/Gross}$-$SoilC_{Ref}$	Pg C	-77.74	-	-	-	-88.96	-11.22

Earth System Dynamics Discussions — Open Access — EGU

Table 3. Changes in C stocks and fluxes in reconstructions of net and gross LUC changes for Europe (EU27+CH). Values are always given as 10-year averages (except LUC areas and cumulative flux).

	Averaging period	Calculation	Unit	HILDA (net)	LUH (net)	Average and uncertainty[a] for the LUC models	HILDA (gross)	difference HILDA (gross-net)
Natural area	1900	A_{nat}	10^6 km^2	1.49	2.16	1.83 ± 0.47	1.49	0
Natural area	2010	A_{nat}	10^6 km^2	2.06	2.79	2.43 ± 0.52	2.06	0
Pasture area	1900	A_{pas}	10^6 km^2	1.62	0.97	1.30 ± 0.46	1.62	0
Pasture area	2010	A_{pas}	10^6 km^2	1.35	0.68	1.02 ± 0.47	1.35	0
Cropland area	1900	A_{crop}	10^6 km^2	1.59	1.57	1.58 ± 0.01	1.59	0
Cropland area	2010	A_{crop}	10^6 km^2	1.29	1.23	1.26 ± 0.04	1.29	0
Total change in natural area	1900-2010	A_{nat}	10^6 km^2	+0.57	+0.63	+0.60 ± 0.04	+0.57	0
Total change in pasture area	1900-2010	A_{pas}	10^6 km^2	-0.29	-0.34	-0.28 ± 0.01	-0.29	0
Total change in cropland area	1900-2010	A_{crop}	10^6 km^2	-0.28	-0.29	-0.32 ± 0.03	-0.28	0
Total area under transition	1900-2010	ΣA_{trans}	10^6 km^2	1.47	1.87	1.67 ± 0.29	2.64	+1.17
E_{LUC}	1900-1909	$E_{LUC\ Net/Gross}$	Tg C a^{-1}	19	38	29 ± 13	29	+9
	1980-1989	$E_{LUC\ Net/Gross}$	Tg C a^{-1}	-25	-78	-51 ± 37	-26	-1
	1990-1999	$E_{LUC\ Net/Gross}$	Tg C a^{-1}	-38	-84	-61 ± 33	-38	0
	2001-2010	$E_{LUC\ Net/Gross}$	Tg C a^{-1}	-52	-80	-66 ± 20	-51	+1
cum(E_{LUC})	1951-1960	$\Sigma E_{LUC\ Net/Gross}$	Tg C	586	1338	962 ± 532	915	+329
	2010	$\Sigma E_{LUC\ Net/Gross}$	Tg C	-936	-1 890	674 ± 48	-531	+406
NPP	1900-1909	$NPP_{Net/Gross}$	Tg C a^{-1}	1464	1 517	1 490 ± 38	1462	-2
	2001-2010	$NPP_{Net/Gross}$	Tg C a^{-1}	2 261	2 361	2 311 ± 71	2243	-18
Change in NPP due to LUC	1900-2010	$NPP_{Net/Gross}-NPP_{Ref}$	Tg C a^{-1}	-30	-10	-20 ± 14	-44	-14
	2001-2010	$NPP_{Net/Gross}-NPP_{Ref}$	Tg C a^{-1}	-57	+10	-23 ± 47	-74	-18
Vegetation C	1900-1909	$VegC_{Net/Gross}$	Tg C	7755	9 634	8 694 ± 1328	7715	-40
	2001-2010	$VegC_{Net/Gross}$	Tg C	10 518	13 484	12 001 ± 2097	10 360	-159
Change in vegetation C due to LUC	1900-2010	$VegC_{Net/Gross}-VegC_{Ref}$	Tg C	-58	-234	-146 ± 125	-199	-141
	2001-2010	$VegC_{Net/Gross}-VegC_{Ref}$	Tg C	+709	+1217	+963 ± 359	+551	-159
Soil C	1900-1909	$SoilC_{Net/Gross}$	Tg C	58 786	60 672	59 729 ± 1334	58 775	-11
	2001-2010	$SoilC_{Net/Gross}$	Tg C	60 016	62 188	59 761 ± 1 536	59 761	-254
Change in soil C due to LUC	1900-2010	$SoilC_{Net/Gross}-SoilC_{Ref}$	Tg C	-199	-314	-256 ± 81	-368	-169
	2001-2010	$SoilC_{Net/Gross}-SoilC_{Ref}$	Tg C	-29	+291	+131 ± 226	-283	-254

[a]note that the uncertainty given here is calculated between 2 values.

850
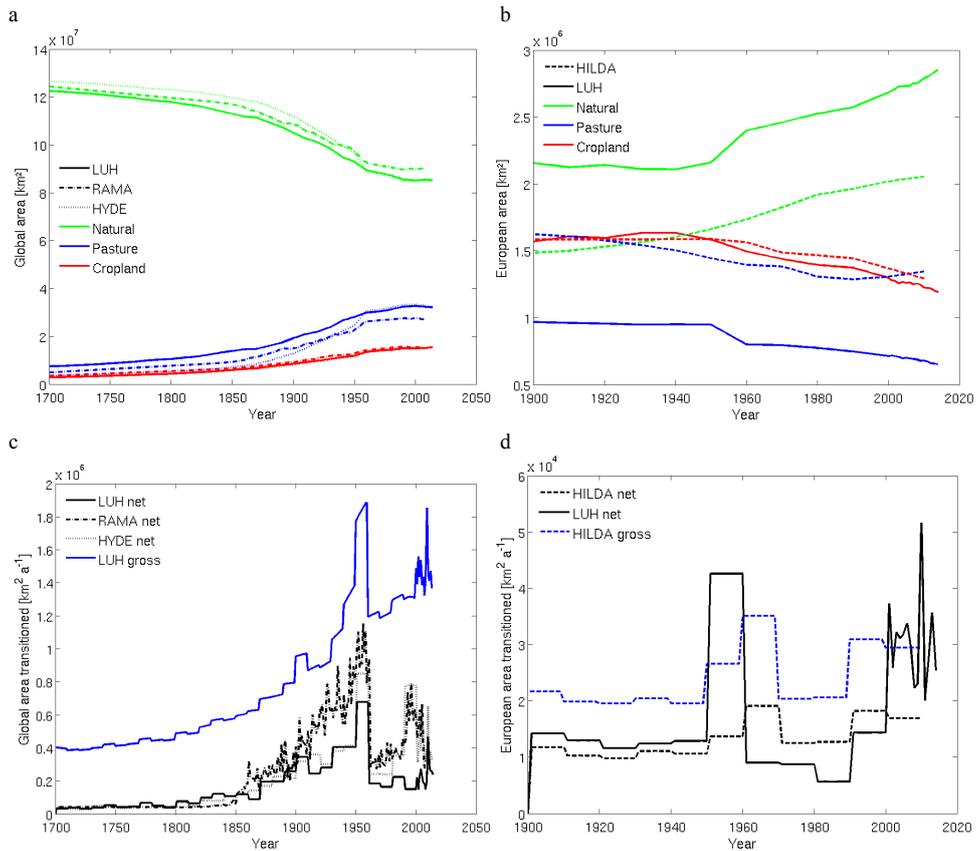
Fig. 1. Land use types and transitions in global and European (EU27+CH) LUC reconstructions. Evolution of
855 absolute land area of croplands, pastures and natural vegetation (including barren land) in different (a) global
historical land use reconstructions (LUH: solid line, RAMA: dash-dotted line, HYDE: dotted line), and (b)
European land use reconstructions (HILDA: dashed line, LUH: solid line). Land area experiencing gross and net
land transitions on global scale (c) and for Europe (d). Note the change to annual resolution in the LUH
reconstruction after the year 2000.

860
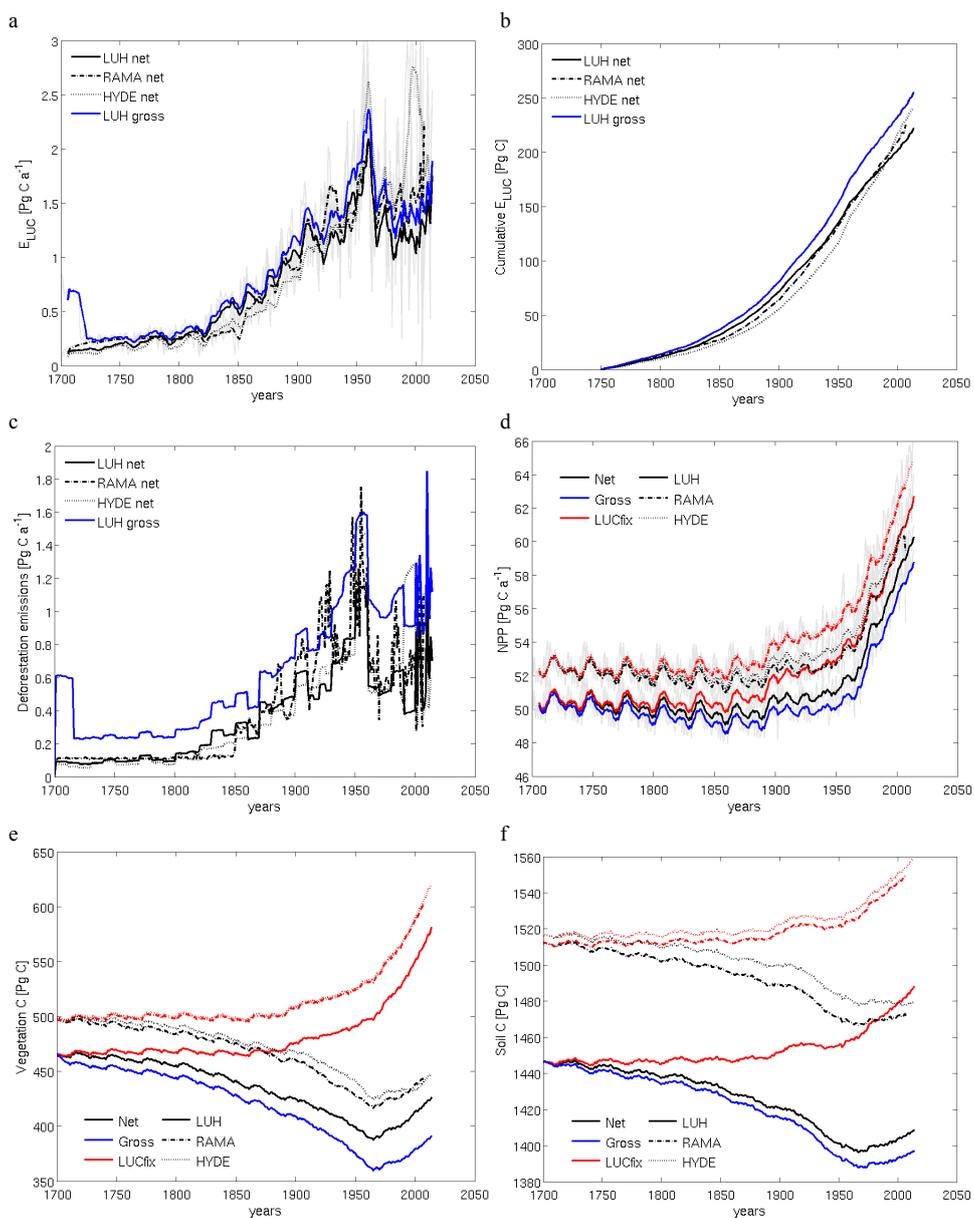
865

Fig. 2. Effects of different land use representations on global ecosystem C stocks and fluxes: Land use flux (a), cumulative land use flux (b), deforestation emissions (c), Net primary productivity (NPP) (d), vegetation (e) and soil carbon stocks (f). Flux values in (a) and (d) are given as 15-yrs averages with original values in the background.

870

875
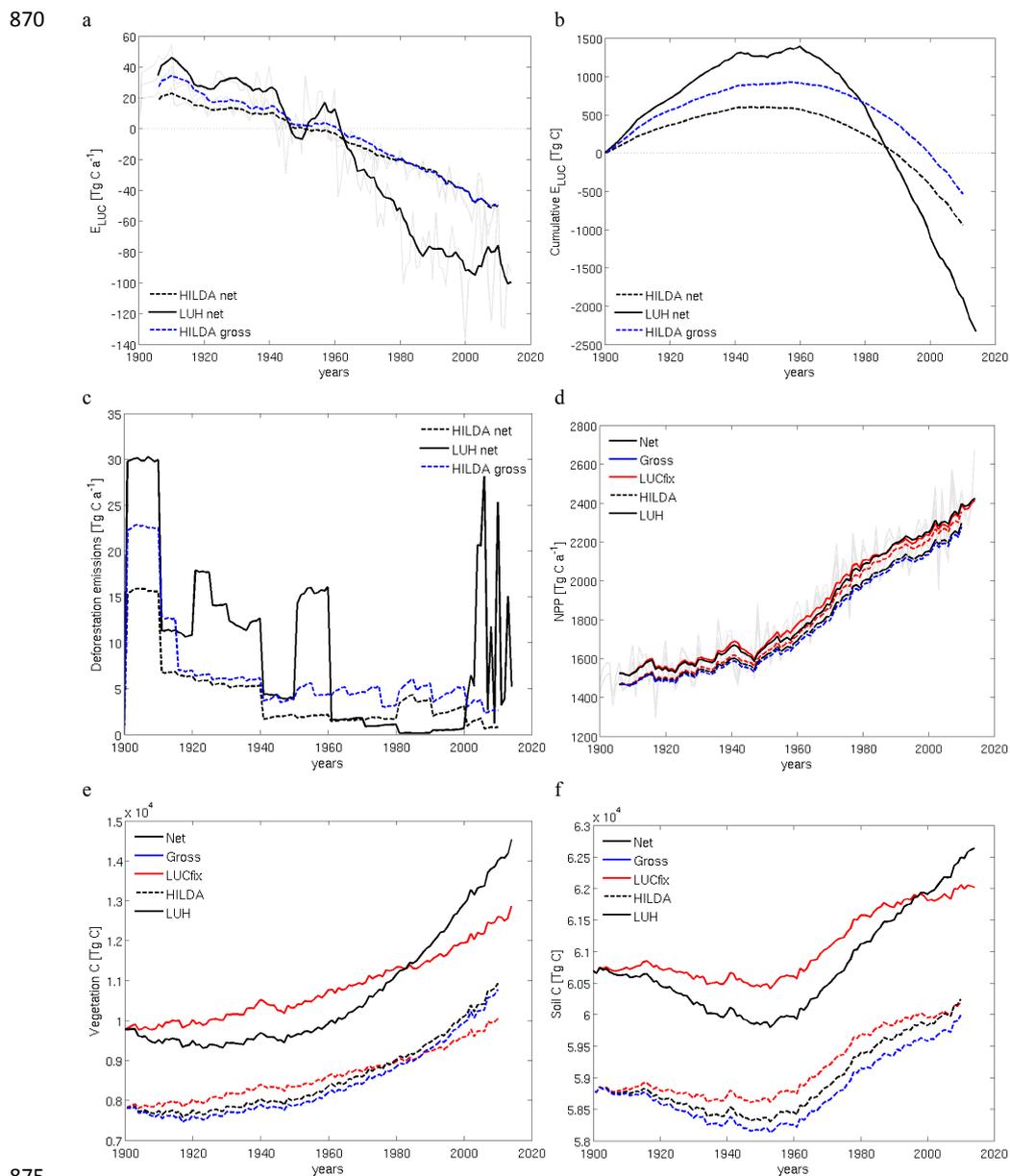
Fig. 3. Effects of different land use representations on ecosystem C stocks and fluxes for Europe (EU27+CH): Land use flux (a), cumulative land use flux (b), deforestation emissions (c), Net primary productivity (NPP) (d), vegetation (e) and soil C (f). Flux values in (a) and (d) are given as 15-yrs averages with original values in the background.

880 a   b
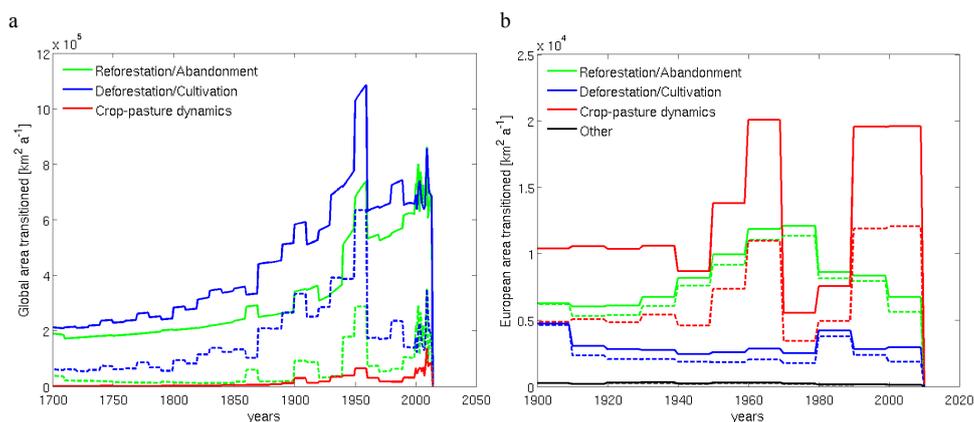
Fig. 4. Annual area transitions for major land change processes for global (a, data from LUH) and European (b, EU27+CH, data from HILDA) gross (solid lines) and net (dashed lines) datasets. The class "other" in (b) includes transitions between natural vegetation and barren land represented in the HILDA dataset.